UC Irvine
UC Irvine Electronic Theses and Dissertations

Title
Mathematical Modeling of CTL Delay and Human Fertility Decline

Permalink
https://escholarship.org/uc/item/90n5s8tk

Author
Stipp, Shaun

Publication Date
2020

Peer reviewed|Thesis/dissertation

eScholarship.org Powered by the California Digital Library
University of California

UNIVERSITY OF CALIFORNIA
IRVINE

Mathematical Modeling of CTL Delay and Human Fertility Decline

DISSERTATION

Submitted in partial satisfaction of the requirements
for the degree of

DOCTOR OF PHILOSOPHY

in Ecology and Evolutionary Biology

by

Shaun Stipp

Dissertation Committee:
Professor Dominik Wodarz, Chair
Professor Matthew Bracken
Professor Anthony Long

TABLE OF CONTENTS

	Page
LIST OF FIGURES	iii
ACKNOWLEDGMENTS	vi
CURRICULUM VITAE	vii
ABSTRACT OF THE DISSERTATION	viii
INTRODUCTION	1
CHAPTER 1: Timing of CD8 T cell effector responses in viral infections	10
CHAPTER 2: The role of mortality and cultural transmission in human fertility decline	29
CHAPTER 3: A continuous model of human fertility decline	56

LIST OF FIGURES

		Page
Chapter 1		
Figure 1	Simulation of model (1)	13
Figure 2	Dependence of minimum virus load on the delay with which effector CTL arrive at the site of the infection, for models (1)-(3)	16
Figure 3	Time-series simulations comparing the dynamics for shorter and longer CTL delays	17
Figure 4	Time series showing the dynamics of (i) infected cells, (ii) unifected target cells (iii) effector CTL over time for model (3)	23
Chapter 2		
Figure 1	Competing populations with only birth/death process	35
Figure 2	Fraction of runs where population h wins in a voter model dynamic with respect to the p_{comm} (frequency with which population h is considered in the voting procedure) and the initial frequency of population l	36
Figure 3	Exclusion/coexistence outcomes of model with both voting and birth/death mechanisms. Nearest-neighbor interactions.	37
Figure 4	Cross-sections of Fig. 3.	38
Figure 5	Time series of three possible outcomes of model with both voting and birth/death mechanisms	38
Figure 6	Exclusion/coexistence outcomes of model with both voting and birth/death mechanisms. Perfect mixing.	39
Figure 7	Cross-sections of Fig. 6.	40
Figure 8	Exclusion/coexistence outcomes of age-structured model with voting and birth/death processes. Nearest-neighbor interactions.	45
Figure 9	Cross-sections of Fig. 8.	46
Figure 10	Exclusion/coexistence outcomes of age-structured model with voting and birth/death processes. Perfect mixing.	47

Figure 11 Cross-sections of Fig. 10. 47

Figure 12 Dynamics of competing age-structured populations as represented by difference equations 50

Chapter 3

Figure 1 Dynamics of average reproduction probability (r_{ave}) for six different death probabilities (p_{death}) assuming endogenous social status and relative weighting 63

Figure 2 Low values of p_{death} result in ever decreasing values in r_{ave} resulting in population crash 64

Figure 3 Long-term average reproduction probability (r_{ave}) with respect to probability of copying error (p_{mut}) in model assuming endogenous social status and relative weighting 64

Figure 4 Long-term average reproduction probability (r_{ave}) with respect to the size of copying error (q) in model assuming endogenous social status and relative weighting 65

Figure 5 Long-term average reproduction probability (r_{ave}) with respect to the rate of transmission ($p_{transmit}$) in model assuming endogenous social status and relative weighting 66

Figure 6 Long-term average reproduction probability (r_{ave}) with respect to the weight of high fertility individuals in the average (a) in model assuming endogenous social status and relative weighting 66

Figure 7 Dynamics of average reproduction probability (r_{ave}) for three different death probabilities (p_{death}) in model assuming endogenous social status and linear weighting 68

Figure 8 Long-term average reproduction probability (r_{ave}) with respect to the rate of transmission ($p_{transmit}$) in model assuming endogenous social status and linear weighting 68

Figure 9 Long-term average reproduction probability (r_{ave}) with respect to s in model assuming endogenous social status and linear weighting 69

Figure 10 Dynamics of the average reproduction probability (r_{ave}) with six different death probabilities (p_{death}) in model assuming decoupled social status and relative weighting 71

Figure 11	Dynamics of average reproduction probability (r_{ave}) for three different rates of transmission ($p_{transmit}$) in model assuming decoupled social status and relative weighting	72
Figure 12	Dynamics of average reproduction probability (r_{ave}) for four different values of *a* in model assuming decoupled social status and relative weighting	73
Figure 13	Dynamics of average reproduction probability (r_{ave}) for different values of w in model assuming decoupled social status and relative weighting	74
Figure 14	Dynamics of average reproduction probability (r_{ave}) for four different death probabilities (p_{death}) in model assuming decoupled social status and linear weighting	75
Figure 15	Dynamics of average reproduction probability (r_{ave}) for different rates of transmission ($p_{transmit}$) in model assuming decoupled social status and linear weighting	76
Figure 16	Dynamics of average reproduction probability (r_{ave}) for different values of w in model assuming decoupled social status and linear weighting	77

ACKNOWLEDGEMENTS

I would like to thank my committee chair and advisor Professor Dominik Wodarz for his patience and loyalty over this long journey.

I would like to thank Professors Matthew Bracken and Anthony Long for their input and service on my committee.

I would also like to express gratitude to my parents for their never-ending support and encouragement.

CURRICULUM VITAE

Shaun Stipp

2015 B.S. in Ecology and Evolutionary Biology, University of California, Irvine

2016-2020 Teaching Assistant, Ecology and Evolutionary Biology, University of California, Irvine

2020 Ph.D. in Ecology and Evolutionary Biology, University of California, Irvine

FIELD OF STUDY

Theoretical Biology, Population Dynamics

PUBLICATIONS

Stipp, S. R., Iniguez, A., Wan, F., Wodarz, D. 2016. Timing of CD8 T cell effector responses in viral infections. R Soc Open Sci. 3: 150661

Wodarz, D., Stipp, S., Hirshleifer, D., Komarova, N. L. 2020. Evolutionary dynamics of culturally transmitted, fertility-reducing traits. Proc Roy Soc B.
DOI: 10.1098/rspb.2019.2468

ABSTRACT OF THE DISSERTATION

Mathematical Modeling of CTL Delay and Human Fertility Decline

By

Shaun Stipp

Doctor of Philosophy in Ecology and Evolutionary Biology

University of California, Irvine, 2015

Professor Dominik Wodarz, Chair

Mathematical and computational models are invaluable tools that enable one to explore the implications of the assumptions one makes about how complex systems operate. In Chapter 1, mathematical models are used to address the question of whether a delay in CTL (cytotoxic T lymphocyte) arrival to the site of an infection can increase the chances of the CTL clearing this infection. The results of three models of increasing complexity imply that there are conditions in which such an advantage of a CTL delay can occur. The mechanism for this advantage as suggested by the models is that as the infection progresses, the virus depletes its source of growth, allowing the CTL to drive the infection to lower levels. In addition, when the rate of CTL activation is proportional to the level of viral antigen, a delay is advantageous in that a higher virus load results in the activation of more CTL. Chapter 2 uses mathematical and computational models to address the phenomenon of human fertility decline. We assume a framework in which two populations—high- and low-fertility—can convert members of the other population into members of its own. We find that when the low-fertility individuals are favored in the conversion process, the low-fertility population can dominate the high-fertility population

when the rate of cultural transmission is high and mortality is low. Chapter 3 investigates the matter of fertility decline in a framework where a continuum of fertilities is possible. Individuals take the weighted average of the fertility of individuals around them with copying error. Outcomes of long-term fertility are investigated with different model assumptions relating to how individuals are assigned a weight in the average. Although the qualitative behavior of the time series of fertility and the influence of parameters on it vary depending on model assumptions, the most general and relevant insight of the models is that long-term fertility is lower under conditions of low mortality.

Introduction

The timing of events in biological systems are relevant to the outcomes of their dynamical processes. For example, theoretical work has shown that delays in development to reproductive maturity can confer a fitness advantage in variable environments, when in constant environments these same life history strategies would incur a fitness cost (Tuljapurkar, 1990). On this note, degrees of iteroparity and semelparity seem to be facultatively adjusted in some circumstances based on the risk of mortality (Baird et al 1986); the woodlouse *Porcellionides pruinosus* has been shown to breed continuously in the tropics, when under temperate conditions it is semelparous (Dangerfield and Telford, 1990); iteroparity, but not fecundity, has been shown to increase in the mosquito *Wyeomyia smithii* as opportunities for blood meals are increased (Bradshaw, 1986); and sea squirts are polymorphic with respect to their life history, with either semelparous or iteroparous dominating the population depending on the season (Grosberg, 1988). In the case of small, isolated populations, subsets of the population may be consigned to breed at different times, a phenomenon known as "cohort splitting" (Willows, 1987).

Delays in the context of space become particularly relevant for processes in the immune system. For example, experiments suggest that in a rechallenge cytotoxic T lymphocytes (CTL) can only effectively extravasate to the peripheral tissues and perform their effector function when newly or persistently stimulated by viral antigen, whereas protection against intravenous injection will be successful without antigen (Kundig *et al.* 1996) The authors hypothesized that the difference in antigen-dependence was due to the time it takes CTL to reach the peripheral tissues. A kinetic analysis of HIV infection has also

shown a delay in CTL expansion, which is believed to be due to CTL requiring minimum antigen levels to mount a response (Davenport et al. 2004). Furthermore, it has been reported that hepatitis C virus outpaces an acute CTL response by several weeks in chimpanzees and this may contribute to viral persistence. Perhaps the most detailed analysis of acute CTL response in both space and time was conducted by Frey et al. (2013), in which a form of in situ hybridization was used to visualize the spread of pneumonia virus of mice (PVM) as well as the CTL response to the infection. In this study, a strong CTL infiltration into the lung occurred only after maximal viral loads were achieved. The authors proposed that such a delay in CTL response may be necessary to ensure effective clearance of the pathogen. The first chapter of this dissertation complements the work of Frey et al. in that a theoretical framework is constructed to model a CTL-mediated clearance of an infection and determine whether and under what conditions a delayed CTL response will be more effective than an early CTL response in clearing the pathogen. Numerical simulations are employed with varying parameter values and amounts of CTL delay. The resulting minima of infected cells are plotted, lower minima corresponding to a greater probability of clearing the infection in the short-term.

Variability of reproductive strategies in response to local conditions is also a defining feature of own species. The nomadic bands of hunter gatherers comprising all of humanity prior to the ninth century B.C.E. would have had a lower fertility than the agricultural societies that followed (Hirchman, 2005; Lawson, 2011; Livi-Bacci, 2017). This fertility schedule would have been characterized by long interbirth intervals maintained via amenorrhea caused by long periods of breastfeeding. Childbearing also started late due to a late age of menarche. Long interbirth intervals and late onset of childbearing is

believed to have been adaptive in a nomadic culture because a woman could only carry one child at a time and the mobility of the band in general would have been impaired by dependent children. The growth of children in these in modern hunter-gatherer societies is also reported to be slow, which is advantageous in that they would be easier to carry.

Then came the Neolithic demographic transition. Agriculture was discovered independently in different societies between 5000 – 8000 B.C.E., and the world experienced a surge in the human population. Early theories proposed that this growth was due to a decrease in mortality and higher birth rate resulting from a more reliable food supply and a consequent improved ability to resist infection. However, it is clear from archeological evidence that mortality was higher among Neolithic farmers than it was in hunter-gatherers. Stature and bone density decreased, and signs of morbidity were abundant. It has been proposed that the higher morbidity and mortality among these populations was due to a less varied diet, depressing overall health and the ability to resist infection. A higher population density also increased the frequency of contacts between people and animals, resulting in a higher transmission rate of disease. Contaminated water supplies did not help in this regard. The fertility rate among these agricultural societies was indeed higher, however. A non-nomadic society relaxed the burden on mothers of having to carry their children, and the agrarian way of life resulted in economic incentives for large families, as even small children could perform basic chores and keep an eye on livestock. It is also reasonable to suggest that some portion of the increase in fertility was a compensation for high mortality.

More recent human history has been characterized by a different sort of demographic transition beginning in the late 18th to early 19th century in Western Europe

and spreading to all corners of the globe in modern times. This transition involves a change from a high fertility and high mortality regime to low fertility and low mortality regime, with the reduction in mortality often preceding the reduction in fertility, especially in countries undergoing the transition more recently (Kirk, 1996). There is disagreement as to the cause of the modest decrease in mortality evident in the 19th century. One proposal is that a greater availability of food supply due to improved farming technology and extensive trade networks enabled individuals to better resist infection (McKeown, 1972). Another scholar has proposed that there was a reduction in infection as a result of cultural practices promoting good hygiene (Razzell, 1974). While this dispute has not been resolved, it is fairly clear that the bulk of increase in lifespan throughout the 20th century is due to the ability to control and treat infectious disease, with a small fraction of the improvement due to increases in income (Preston, 1976).

Explanations for the reduction in fertility have been more elusive than those for mortality. Early theories posited that fertility reduction resulted from changes in lifestyle accompanying development, but these classical theories have little support in that only modest correlations between historical fertility and measures of development have been found (Knodel and van de Walle, 1979; Notestein, 1945; Thompson, 1929). Moreover, regions undergoing a fertility reduction more often shared more in common with respect to language and culture than with respect to development. As a result, some scholars advanced ideational theories of fertility decline, which propose that changes in social values result in an overall lower rate of fertility (Cleland and Wilson, 1987; Lesthaeghe, 1983), while other scholars propose a complex interaction between socio-economic circumstances and ideational factors (Mason, 1997).

Fertility reduction observed in developed countries displays a consistent diffusion pattern throughout the society and has been characterized by distinct changes in fertility tempos over time. As countries undergo a fertility transition, the social elites are usually observed to reduce their fertility first (Knodel and van de Walle, 1979). This relationship between social class and fertility persists in some form today, as null or negative relationships are often observed between fertility and measures such as education and income (Vining, 1986). In the first societies to undergo the demographic transition, fertility reduction frequently took the form of family limitation, where reproduction was stopped once a desired number of children had been reached (Knodel and van de Walle, 1979). In the twentieth century, fertility reduction in developed societies takes the form of later ages at first birth, largely attributable to the increases in years of educational participation (Cohen et al 2011).

The reduced fertility in modern societies has been discussed in evolutionary terms. It at first seems strange that humans appear to be reducing their fertility during times of abundant resources. An easy resolution to the dilemma might be expected in theories related to optimal clutch size (Lack, 1947). Such theories state that intermediate numbers of offspring will pay off in future generations, as parents can invest more in few offspring than in many, which will translate into greater survival and reproduction. Unfortunately, researchers employing this methodology have failed to find any evidence of a quantity-quality tradeoff in humans, in terms of fitness (Kaplan et al 1995; Kaptijn et al 2010). Other researchers invoke an adaptive lag hypothesis, which states that the modern environment is different from the ancestral environment in such way that psychic and behavioral traits which used to translate into maximal fitness are no longer operating to this end (Alvergne

and Lummaa, 2014; Perusse, 1993). Still another faction claims that modern fertility reduction is explicable via evolutionary but non-genetic modes of inheritance (Boyd and Richerson, 1985; Cavalli-Sforza and Feldman, 1981; Fogarty et al., 2013; Ihara and Feldman, 2004). The second and third chapters of this dissertation employ this last approach to explain the key features of the demographic transition. In the second chapter, individuals belong to either a high- or low-fertility population, each of which can convert members of the other population into members of its own. Competition outcomes are observed for various rates of conversion, levels of social status, and rates of exogenous mortality. The third chapter investigates the evolutionary dynamics of fertility as a continuous, culturally transmitted trait and investigates the role of social status in its transmission. Outcomes are observed for various values of copying error, error quantity, rates of transmission, costs of reproduction on status, and mortality.

References

Alvergne, A., Lummaa, V. 2014. Ecological variation in wealth-fertility relationships in Mongolia: the central theoretical problem of sociobiology not a problem after all. *Proc Biol Sci* 281(1796):20141733.

Baird, D. J., Linton, L. R., Davies, R. W. 1986. LIfe-history evolution and post reproductive moratility risk. *Journ An Ecol* 295-302.

Boyd, R., Richerson, P. 1985. *Culture and the Evolutionary Process.* Chicago: University of Chicago Press.

Bradshaw, W. E. 1986. Variable iteroparity as a life-history tactic in the pitcher-plant mosquito Wyeomyia Smithii. *Evolution* 40(3):471-478.

Cavalli-Sforza, L. L., Feldman, M. W. 1981. *Cultural Transmission and Evolution: A Quantitative Approach.* Princeton: Princeton University Press.

Cleland, J., Wilson, C. 1987. Demand theories of the fertility transition: an iconoclastic view. *Pop Stud* 41(1):5-30.

Cohen, J. E., Kravdal, O., Keilman, N. 2011. Childreaing impeded education more than education impeded childbearing among Norwegian women. *Proc Natl Acad Sci U S A* 108(29):11830-11835.

Dangerfield, J. M., Telford, S. R. 1990. Breading phenology, variation in reproductive effort and offspring size in a tropical population of the woodlouse Prcellionides pruinosus. *Oecologia* 82:251-258.

Davenport, M. P., Ribeiro, R. M., Perelson, A. S. 2004. Kinetics of virus-specific CDi+ T cells and the control human immunodeficiency virus infection. *Journ Virol* 78(18):10096-10103.

Fogarty, L., Creaenza, N., Feldman, M. W. 2013. The role of cultural tranmission in human demographic change: an age-structured model. *Theor Pop Biol* 88:68-77.

Frey, S., Pircher, H., Follo, F., Collins, P., Krempl, C., Ehl, S. 2013. In situ evolution of virus-specific cytotoxic T cell responses in the lung. *Journ Virl* 87(20):11267-11275.

Grosberg, R. K. 1988. Life-history variation within a population of the colonial ascidian

Botryllus Schlosseri. I. The genetic and environmental control of seasonal variation. *Evolution* 42(5):900-920.

Hirschman, C. 2005. Population and Society: Historical Trends and Future Prospects. In *The Sage Handbook of Sociology*, by C., Rojek, C., Turner, B. S. Calhoun, 381-402. London: Sage Publications.

Ihara, Y., Feldman, M. W. 2004. Cultural niche construction and the evolution of small family size. *Theor Pop Biol* 65:105-111.

Kaplan, H. S. et al. 1995. Fertility and fitness among Albuquerque men: a competitive labour market theory. In *Human Reproductive Decisions*, by R.I.M., ed. Dumbar, 96-136. St. Martin's Press.

Kaptijn, R. Thomese, F. van Tilburg, T. G., Liefbroer A. C., Deeg, D. J. H. 2010. Low fertility in contemporary humans and the mate value of their children: sex-specific effects on social status indicators. *Evolution and Human Behavior* 31:59-68.

Kirk, D. 1996. Demographic transition theory. *Pop Stud* 50(3):361-387.

Knodel, J., van de Walle, E. 1979. Lessons from the past: policy implications of historical fertility studies. *Popul and Devel Rev* 5(2):217-245.

Kundig, T. M., Bachmann, M. F., Oehen, S., Hoffmann, U. W., Simard, J. J., Kalberer, C. P., Pircher H., Ohashi, P. S., Hengartner, H., Zinkernagel, R. M. 1996. On the role of antigen in maintaining cytotoxic T-cell memory. *Proc Natl Acad Sci U S A* 93(18):9716-9723.

Lack, D. 1947. The significance of clutch size. *Ibis* 89(2):302-352.

Lawson, D. W. 2011. "Life History Theory & Human Reprductive Behavior." In *Evolutionary Psychology: A Critical Introduction*, by V. Swami. Oxford: Wiley-Blackwell.

Lesthaeghe, R. A. 1983. A century of demographic and cultural change in Western Europe: an exploration of underlying dimensions. *Popul Dev Rev* 9:411-435.

Livi-Bacci, M. 2017. A Concise History of World Population. 33-42. New Jersey: Wiley/Blackwell.

Mason, K. O. 1997. Explaining fertility transitions. *Demography* 34(4):443-454.

McKeown, T. 1972. An interpretation of the mdoern rise of population in Europe. *Pop Stud* 26(3):345-382.

Notestein, Frank W. 1945. "Population - the long view." In *Food for the World*, by T.W. Schultz. ed., 36-57. Chicago: University of Chicago Press.

Perusse, D. 1993. Cultural and reproducctive succes in industrial societies: test relationships at the proximate and ultimate levels. *Behav Brain Sci* 16:267-322.

Preston, S. 1976. "Mortality Patterns in National Populations." Ch. 4. New York: Academic Press.

Razzell, P. 1929. "An interpretation of a modern rise of population in Europe: a critique." *Pop Stud* 28(1):5-17.

Thompson, W. 1929. "Population." *Am Journ of Sociol* 34:959-75.

Tuljapurkar. 1990. "Delayed reproduction and fitness in variable environments." *Proc Natl Acad Sci USA* 1139-1143.

Vining, D. R. 1986. "Social versus reproductive success--the central theoretical problem of human sociobiology." *Behav Brain Sci* 9:167-260.

Willows, R. I. 1987. "Population dynamics and life history of two contrasting populations of Ligia oceanica (Crustacea: oniscidea) in the rocky supralittoral." *Journ Anim Ecol* 56:315-330.

Chapter 1: Timing of CD8 T cell effector responses in viral infections

1.1 Introduction

CD8+ T cells, or cytotoxic T lymphocytes (CTL), represent an important branch of the immune system in the control and clearance of viral infections. The role of CTL in the management of infections has been studied in detail for human pathogens such as human immunodeficiency virus (HIV) (Leslie et al 2004; Goulder and Watkins, 2004; Rowland-Jones et al 1997; Asquith and McLean, 2007) and hepatitis B (Maini et al 2000; Guidotti et al 1999; Sobao et al 2002) and C viruses (Nelson et al 1997: Timm et al 2004; Lechner 2000; Moskophidis et al 1997). They can induce lysis of infected cells, or shut down the replication of viruses within infected cells via soluble mediators (Levy et al 1996; Seich Al Basaten et al 2013). While they serve a positive role in this respect, they can also negatively affect the organism in a phenomenon called "CTL-induced pathology" (Zinkernagel and Hengartner, 1994), which occurs when the CTL destroys tissue sufficiently to cause disease. The correlates of CTL-mediated control and CTL-induced pathology have been studied in much detail (Guidotti and Chisari, 2006)

There is literature which suggests the rate at which CTL respond to viral antigen has an important role in how effectively they can control virus replication and limit pathology. In one instance, LCMV-specific CTL failed to protect the animals against peripheral re-challenge, yet they were successful against intravenous infection (Kundig et al 1996). The authors of this study proposed that the time it takes for CTL to reach the peripheral tissues was responsible for this observation. A delay in HIV response was also found in a kinetic

analysis of data from an HIV vaccine trial (Davenport et al 2004). In this case, the authors of the study proposed that viral antigen needed to reach a certain level before CTL could respond to the infection. The most detailed analysis of the kinetics of acute CTL responses, however, was conducted by Frey (2013). Using in situ hybridization techniques to visualize the spread of PVM and its CTL response in space and time, they found that CTL infiltrated the lungs only after maximal viral loads had been achieved, which coincided with the manifestation of symptomatic disease. The authors hypothesized that such a CTL delay was necessary to ensure effective CTL-mediated clearance of the infection. If this claim is true, it will have great implications for CTL-based vaccination approaches, as such vaccines are often designed to accelerate CTL effector activity with the aim of minimizing pathology (Davenport et al 2007).

Given that the development of maximal CTL mediated activity can take time during which the virus infection can spread to target tissue, strategies designed to accelerate CTL effector activity are discussed in the literature, especially in the context of vaccination approaches. This project instead operates on the hypothesis that a delay in CTL effector activity can be more effective at clearing an infection. Mathematical models were employed that investigated the effectiveness of CTL to clear an infection under different conditions, including amounts of CTL delay. It was found that a delayed CTL effector response can be more likely to clear an infection than an early response under certain conditions. Although a delayed CTL effector response could come at the cost of CTL-induced pathology, a greater likelihood to clear an infection might be the greater selective pressure. Thus an inherent delay in CTL-mediated anti-viral activity might be adaptive. These models are used to

interpret experimental data summarized above, in particular that of Frey *et al* (2013), which motivated our work.

1.2 Results

1.2 i. The Simplest Model

This project used a modified version of a familiar system of ordinary differential equations.

$$\frac{dS}{dt} = \lambda - dS - \beta SI$$

$$\frac{dI}{dt} = \beta SI - aI - kIZ \qquad (1)$$

$$\frac{dZ}{dt} = -bZ$$

Susceptible target cells, infected cells, and CTL are represented by variables S, I, and Z, respectively. Susceptible cells are produced at a rate λ, die at a rate d, and are converted to infected cells at a rate β. The free virus load is assumed to be proportionate to the level of infected cells, which is justified if the rate of virus production is much greater than the rate of infected cell production. Infected cells have an inherent death rate of a and are killed upon encountering CTL at a rate k. CTL die at a rate b. The properties of basic virus

dynamics equations are well defined in the literature (Novak and May, 2000). An important quantity is the basic reproductive ratio, which needs to be greater than 1 for the virus to establish a successful infection. We set the initial number of CTL as $Z(0) = 0$, and then introduced a number of CTL at varying time thresholds $Z(t=T_{thr})$. **Fig.1.** gives the dynamics produced by this framework. The continued stimulation of CTL by antigen is not considered in this model for simplicity, thus the CTL are not maintained in the long-term, and the infected cell population will eventually grow back. We are interested in the short-term infection dynamics, as the lower the minimum level of infected cells in this phase, the greater the likelihood of clearing the infection. Note that the concentration of cells is being modeled, not their number, so a population size of 1 would not represent extinction.

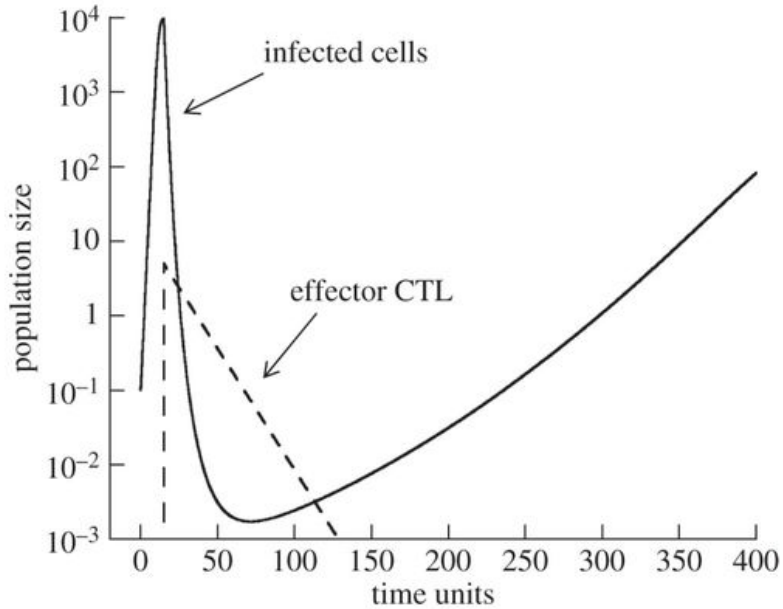

Fig. 1. Simulation of model (1). The virus population is depicted by the solid line, the effector CTL by the dashed line. Virus growth starts at time zero, and the CTL population is introduced at a later time point. Upon introduction of the CTL, the virus population declines. Owing to the simplicity of the model, the CTL population also declines and is not

maintained in the long-term. Following the CTL decline, the virus population re-grows. The minimum virus load achieved by CTL-mediated activity is a measure of the effectiveness with which the acute CTL reduce virus load. We examine how this minimum depends on the timing of CTL introduction under different parameter regimes. Parameters were chosen as follows: Lambda = 1, d = 0.0001, Beta = 0.001, a = 0.0002, b = 0.75, k = 0.25. Initial conditions were as follow: S(0) = lambda/d, I(0) = 0.1.

Fig. 2a. plots minima as a function of the amount of delay for different parameter regimes. β is varied left-to-right, as the parameter was shown through numerical simulations to have the greatest effect on the relationship between CTL introduction time and minimum number of infected cells. The purpose is not to model a specific infection, hence, parameters are simply chosen to demonstrate the possibility of an advantageous delay in CTL response.

At high rates of virus replication, increased CTL delays result in monotonically decreasing minima of infected cells (**Fig. 2a (i)**). At high rates of viral replication and long CTL delays, the virus more completely depletes its source of growth, the target cells (**Fig. 3a**). A lower availability of target cells results in a faster decline in the infected cell population in the presence of CTL, thus resulting a lower minimum infected cell population. This is despite the fact that there is a higher level of infected cells to depress at high rates of infection and long CTL delays. At intermediate levels of virus replication, a minimum amount of CTL delay is required for the effect of the virus depleting its source of growth to outweigh its resistance to being depressed from high levels. This results in the one-hump pattern observed in **Fig. 2a (ii)**. At even lower virus replication rates, an even greater amount of delay is necessary for this tradeoff to be observed (**iii**). Although beyond a certain amount of delay target cells are depressed sufficiently to result in lower minima, an absence of any CTL delay is more effective in this regime. The rate of target production, λ,

also has an effect on the ability of CTL to clear the infection with long delays, as shown in the dashed line of **Fig. 2a (ii)**. The target cell population is not reduced by the virus as easily at high rates of production, thus reducing the effectiveness of a delay in reducing the level of infected cells. In this simulation, the rate of d is also adjusted such that the initial tissue size is the same as in the solid line.

To summarize, the effectiveness of a delayed CTL response in clearing the infection is dependent on how effective the virus is at the depleting the target cell population. It is more difficult for CTL to reduce the infected cell population from high levels resulting from high rates of infection and extended CTL delays than it is for the CTL to reduce the infected cell population from lower levels. However, high rates of infection and greater CTL delays result in a more depleted target cell population, which enhances the ability of CTL to reduce the infected cell population. There is therefore a tradeoff that arises. In the parameters regimes investigated, a CTL delay is more effective at clearing the infection when the rate of infection is sufficiently high.

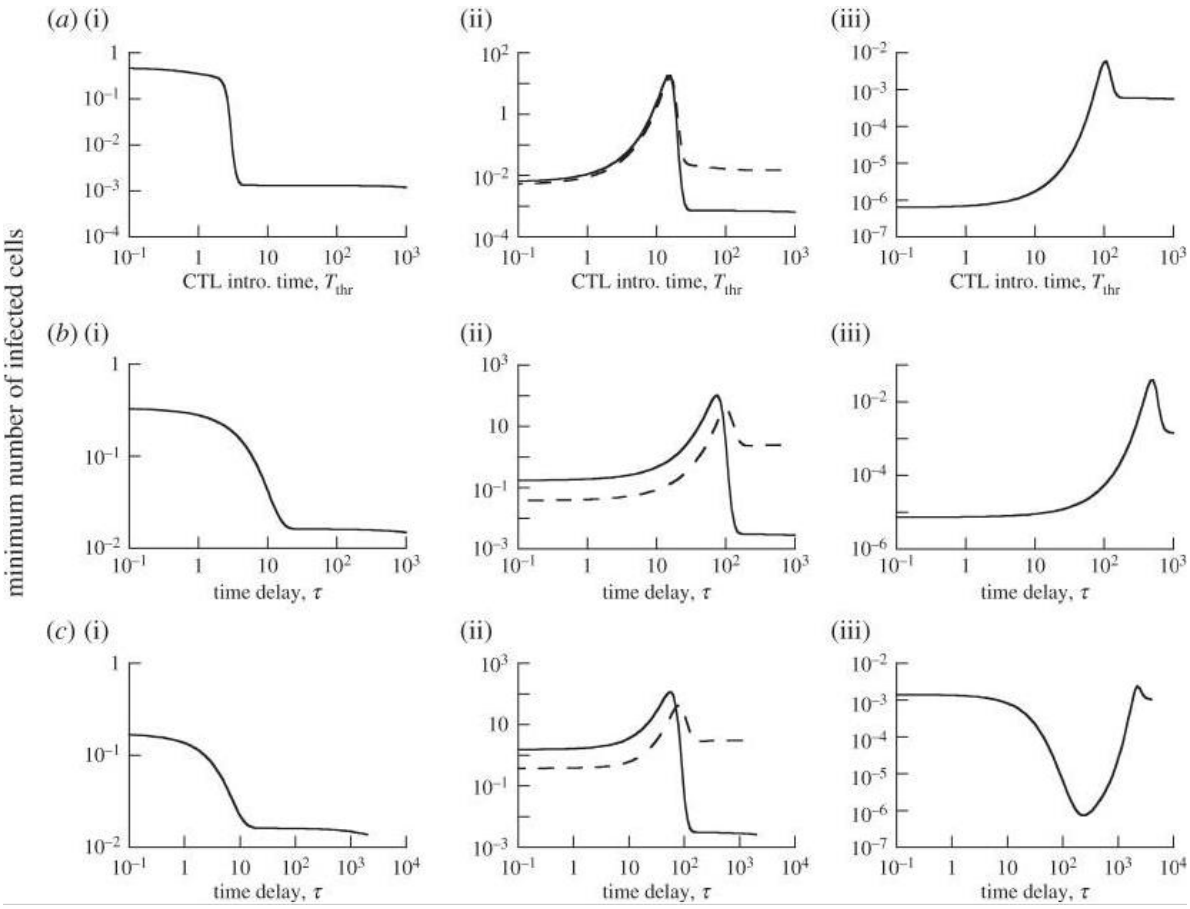

Fig. 2. Dependence of minimum virus load on the delay with which effector CTL arrive at the site of the infection, for models (1)-(3). For each delay (or CTL introduction time), the models were simulated, giving rise to a time series similar to the one seen in **Fig. 1.** The minimum virus load was determined and plotted. (a) Model (1), (b) model (2) and (c) model (3). For a-c, panels (i)-(iii) show the dependence for different parameter combinations. A dashed curve in some of the graphs shows the dependence for an increased turnover rate of the target cell population, with other parameters remaining identical. Specifically, the parameters were chosen as follows. (a) $\lambda = 1$, $d = 0.0001$, $a = 0.0002$, $b = 0.075$, $k = 0.25$. Upon introduction, $Z = 5$. (a(i)) $\beta = 0.0004$; (a(ii)) $\beta = 0.00006$, dashed line: $\lambda = 100$, $d = 0.01$; (a(iii)) $\beta = 0.00001$. (b) $\lambda = 1$, $d = 0.0001$, $a = 0.0002$, $b = 0.075$, $k = 1$, $a = 0.5$, $g = 0.01$, $r = 1$. (b(i)) $\beta = 0.00005$; (b(ii)) $\beta = 0.00001$, dashed line: $\lambda = 100$, $d = 0.01$; (b(iii)) $\beta = 0.000002$. (c) Basic parameter same as for (b), with the parameters $p = 1$, $u = 1$, $u_0 = 1$, $\eta = 0.5$. (c(i)) $\beta = 0.00005$; ((ii)) $\beta = 0.00001$, dashed line: $\lambda = 100$, $d = 0.01$; (c(iii)) $\beta = 0000005$. The initial conditions were as follows: $S(0) = \lambda/d$, $I(0) = 0.1$, $R(0) = 0.2$, $V(0) = V_0(0) = 0$. All other variables were set to 0.

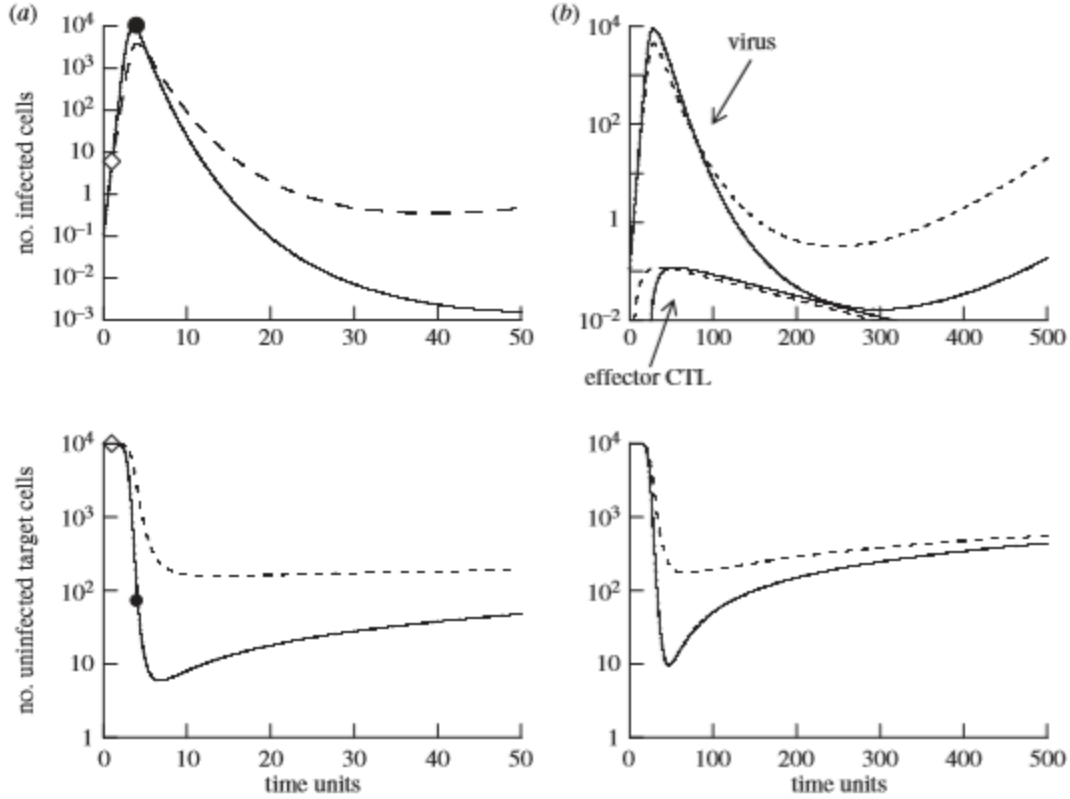

Fig. 3. Time-series simulations comparing the dynamics for shorter (dashed line) and longer (solid line) CTL delays. (a) Simulation of model (1). The diamond symbol indicates the point at which the CTL population is introduced for the short delay scenario, and the circle indicates the CTL introduction time for the longer delay scenario. (b) Simulation of model (2). The upper panel that shows the virus load curves also shows the dynamics of the CTL effector populations, as this model explicitly describes clonal expansion. Parameters were chosen as follows. (a) $\lambda = 1$, $d = 0.0001$, $\beta = 0.0004$, $a = 0.0002$, $b = 0.075$, $k = 0.25$. Initial conditions: $S(0) = \lambda/d$, $I(0) = 0.1$. (b) $\lambda = 1$, $d = 0.0001$, $\beta = 0.00005$, $a = 0.0002$, $b = 0.075$, $k = 1$, $\alpha = 0.5$, $g = 0.01$, $\eta = 0.5$, $r = 1$. Initial conditions: $S(0) = \lambda/d$, $I(0) = 0.1$, $R(0) = 0.2$, $V(0) = V_o(0) = 0$. All other variable were set to zero.

1.2 ii. Model with Clonal Cytotoxic T Lymphocyte Expansion and Migration

Here a more realistic model is explored in which the clonal expansion of CTL as well as the migration of CTL from the lymphoid tissue to the site of infection are explicitly modeled. The processes by which CTL responses are initiated remains incompletely understood, and

there is disagreement about how this process should be described mathematically. In the models below, the simplest process comparable to the model in the previous section is explored—that is, CTL start to undergo rounds of programmed proliferation in the presence of any amount of viral antigen in the lymphoid tissue, and these rounds of replication do not depend on further antigenic stimulation. One should note that the rate of CTL activation in this model is not proportional to the amount of antigen present in the lymphoid tissue. CTL activation is assumed to happen with a constant rate regardless of antigen concentration, as long as antigen is present. This is an unrealistic assumption that represents the next layer of complexity in the model. In the next section, we will explore a model in which the rate of CTL activation is proportional to the amount of antigen. The model is given by the following set of ordinary differential equations:

$$\left.\begin{aligned}
\frac{\mathrm{d}S}{\mathrm{d}t} &= \lambda - dS - \beta SI, \\
\frac{\mathrm{d}I}{\mathrm{d}t} &= \beta SI - aI - kIE, \\
\frac{\mathrm{d}R}{\mathrm{d}t} &= -\alpha R, \\
\frac{\mathrm{d}A_0}{\mathrm{d}t} &= \alpha R - rA_0, \\
\frac{\mathrm{d}A_i}{\mathrm{d}t} &= 2rA_{i-1} - rA_i, \\
\frac{\mathrm{d}A_n}{\mathrm{d}t} &= 2rA_{n-1} - gA_n \\
\frac{\mathrm{d}E}{\mathrm{d}t} &= gA_n(t-\tau) - bE.
\end{aligned}\right\} \qquad (2)$$

As before, the number of susceptible CTL are represented by S, and the number of infected CTL are represented by I. R represents the number of resting CTl at the start of the infection. Resting CTL become activated at a rate α, and activated CTL proliferate at a rate r.

The factor 2 comes from the division of cells. After the final division, activated CTL differentiate into effector CTL, represented by E, at a rate g. These effector CTL then arrive at the site of infection after a certain some delay, denoted by τ. Thus this is a delay differential equation, implemented using Matlab. As in the previous model, this model only examines the acute phase of the infection. There is no sustained CTL activity in response to viral antigen, and thus the level of infected cells will eventually grow back. The value of the minimum virus load again correlates with the likelihood to clear the infection.

The results of this model are highly comparable to those of the previous model. **Fig. 3b** illustrates the mechanism behind these results. At high rates of virus replication, a delay in CTL response will always result in a lower level of infected cells during the acute response to the infection (**Fig. 2b (i)**), resulting in a higher likelihood of virus clearance. At intermediate rates of virus replication, the amount of CTL delay must cross a certain threshold for the effect of reducing the number of target cells to overcome the difficulty of reducing infected cells from high levels (**Fig. 2b (ii)**). At low rates of virus replication, although a reduced target cell load will eventually outweigh the effect a high virus load at high CTL delays, it is better for the CTL to initiate an early response than a later response (**Fig. 2b (iii)**). As before, a lower level of infected cells corresponds to a greater likelihood to clear the infection.

1.2 iii. Antigen-driven expansion of Cytotoxic T Lymphocyte

In the previous model, it was assumed that any amount of viral antigen would activate resting CTL and that the rate of the activation did not depend on level of antigen. Here, it is

assumed that the amount of resting CTL recruitment is proportionate to the amount of viral antigen in the lymphoid tissue. In accordance with data, it is assumed that the rate of CTL proliferation and division after recruitment is determine by a program not dependent on the amount of viral antigen. This model includes two additional values: the amount of viral antigen present at the site of the infection, V, and the amount of viral antigen present in the lymphoid tissue, V_0. These variables do not represent the amount of replicating virus but the amount viral antigen displayed on antigen presenting cells. The model is given by the following system of ordinary differential equations:

$$\left.\begin{aligned}
\frac{\mathrm{d}S}{\mathrm{d}t} &= \lambda - dS - \beta SI, \\
\frac{\mathrm{d}I}{\mathrm{d}t} &= \beta SI - aI - kIE, \\
\frac{\mathrm{d}V}{\mathrm{d}t} &= pI - uV - \eta V, \\
\frac{\mathrm{d}V_0}{\mathrm{d}t} &= \eta V - u_0 V_0, \\
\frac{\mathrm{d}R}{\mathrm{d}t} &= -\alpha R V_0, \\
\frac{\mathrm{d}A_0}{\mathrm{d}t} &= \alpha R V_0 - rA_0, \\
\frac{\mathrm{d}A_i}{\mathrm{d}t} &= 2rA_{i-1} - rA_i, \\
\frac{\mathrm{d}A_n}{\mathrm{d}t} &= 2rA_{n-1} - gA_n \\
\frac{\mathrm{d}E}{\mathrm{d}t} &= gA_n(t-\tau) - bE.
\end{aligned}\right\} \qquad (3)$$

Viral antigen at the site of infection is produced by infected cells with a rate p, decays with a rate u, and is transported to the lymphoid tissue with a rate η. Viral antigen in the lymphoid tissue decays with a rate u_0, which may relate to the dissociation of viral antigen from the surface of APCs. The CTL activation, proliferation and differentiation process is

similar to model (2). The difference is that now the rate of CTL activation is proportional to the amount of viral antigen in the lymphoid compartment. The number of effector CTL at the site of infection is given by E and occurs with a time delay τ. Note that although CTL recruitment is proportional to the level of viral antigen, only the initial program of CTL proliferation and differentiation is modeled, not the sustained stimulation of CTL. Thus only the acute infection dynamics are considered, as in the previous two models, where CTL arrive at the site of infection, perform effector activity, and die.

In the previous models, two main factors determined the effectiveness of CTL to drive the virus to low levels. The first is the level of infected cells present when CTL arrive at the site of the infection. The second is the level of target cells present as a source of growth for the virus. While a CTL delay would allow the virus to rise to higher levels, thus making clearance more difficult, such a delay would also allow the virus to more completely deplete their source of growth, the target cells. A depleted target cell population results in a faster rate of infected cell decline in the face of CTL and a greater likelihood of clearing the infection. In this third model, there is an additional factor which determines the effectiveness of CTL to clear the infection: The rate at which resting CTL are stimulated by viral antigen. An early CTL response might not be effective at clearing the virus, as early in the infection, the level of infected cells is low, and fewer CTL will have been recruited to fight the pathogen. CTL will be more stimulated by higher levels of the pathogen later in the infection and thus more likely to clear the virus. In this model, the effect of a CTL delay on the infection dynamics represents a balance of all three processes described above.

In this model, any amount of CTL delay is advantageous in clearing the infection when the rate of viral replication is high (**Fig. 2c (i)**). This result is comparable to the

previous two models. However, there are two potential mechanisms for this observation, possibly occurring at the same time. 1) Later CTL delays result in a reduced target cell population, resulting in a higher rate of decline in the infected cell population upon introduction of CTL (**Fig. 4a (ii)**). 2) Long CTL delays result in a higher infected cell population, which stimulates the CTL into recruitment at a higher rate than in short CTL delays. (This is not shown in **Fig. 4a**, but can be observed.) As shown in **Fig. 2c (ii)**, the results of intermediate rates of viral replication are comparable to those in the previous models and explained via the same mechanism. At first, a longer CTL delay results in a higher minimum level of infected cells. Then even longer delays result in lower minima of infected cells. This pattern is observed because the effect of a depleted target cell population outweighs the positive effect of higher infected cell populations at sufficient amounts of delay. In this regime, the size of the CTL population as it kills the virus is not significantly effected by the delay (**Fig. 4b(iii)**). As in the previous models, the rate of tissue turnover can influence the effect of a CTL delay (**Fig. 2c(ii)**, solid versus dashed line). Very low rates of viral replication produce a qualitatively different outcome than what was observed in the previous two models (**Fig. 2c(iii)**). The minimum level of infected cells at first decreases dramatically with longer CTL delays. Then with further CTL delay, this effect is reversed. Although higher levels of infected cells are achieved with longer CTL delays, the magnitude of the CTL response is higher in response to larger infected cell populations (**Fig. 4c**), thus enhancing the CTL's ability to clear the infection. The effect of greater antigenic stimulation on the size of a CTL response is observable in this parameter regime and not others because the rate of infection is low. At low rates of infection, CTL delays have a greater effect on the infection to grow to certain levels. This effect is eventually

reversed because beyond a threshold level of infected cells, all available CTL are used, and therefore higher minima result due to the CTL having to reduce greater populations of infected cells. Although the population of target cells is more reduced at longer CTL delays, the effect of this process is outweighed by the high level of infected cells.

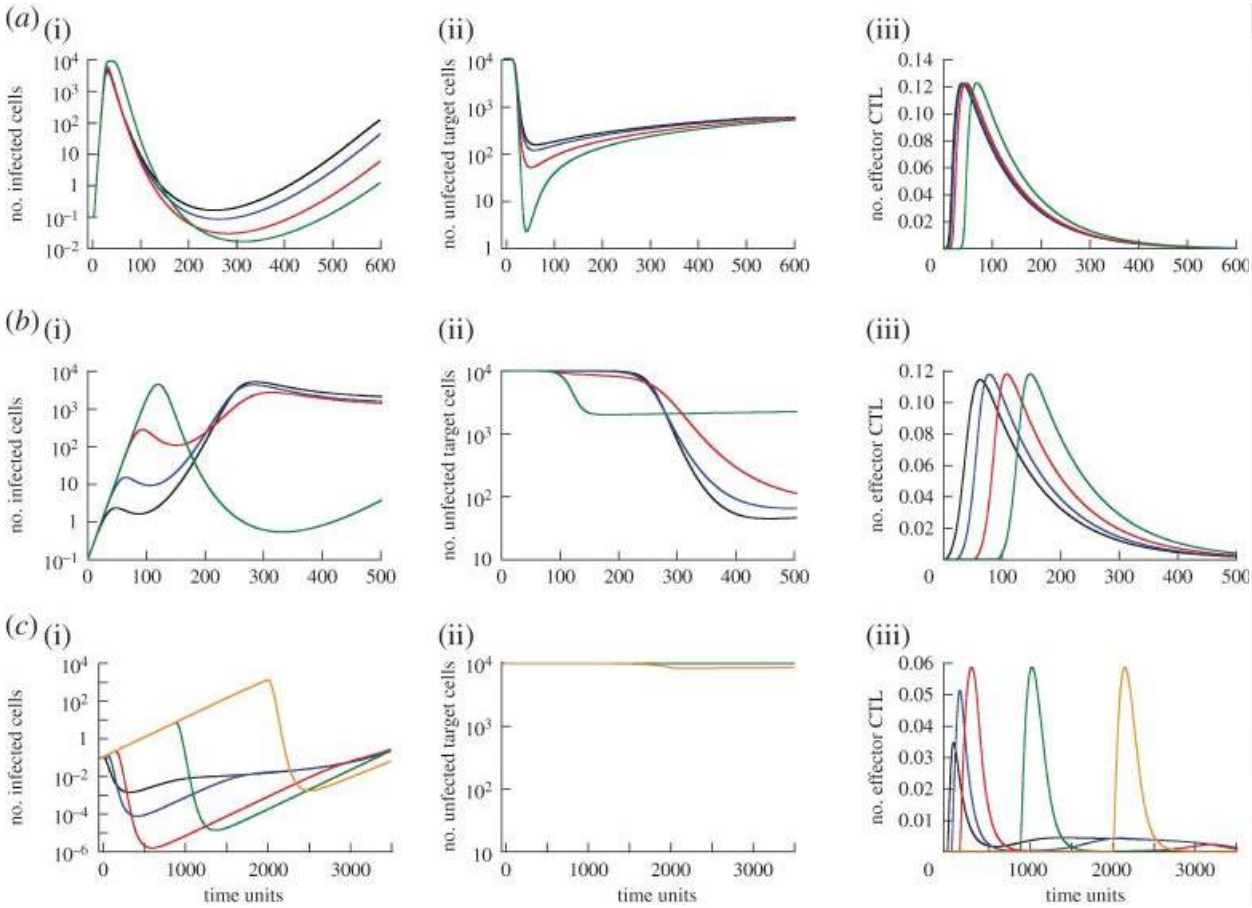

Fig. 4. Time series showing the dynamics of (i) infected cells, (ii) uninfected target cells and (iii) effector CTL over time for model (3). Panels (a-c) correspond to the parameter regimes in **Fig. 2c(i)-(iii)**. The different colored curves in each graph represent different CTL delay times. Colors going from shortest to longest delay time are as follows: black, blue, red, greed, orange. These graphs illustrate the reason for the dependencies seen **Fig. 2c**. See text for details. For parameter values and initial conditions, see **Fig. 2**.

1.3 Discussion

The numerical simulations investigated in this study show that the relationship between the timing of CTL responses and their ability to reduce virus load during acute infections is not straightforward. Under a wide range of parameter regimes, a delay in a CTL response can result in lower levels of infected cells and thus a greater chance of clearing the infection. This is due to the fact that when CTL delay, infected cells reach higher levels. This results in a greater depletion of target cell and/or a higher rate of CTL activation, both of which cause a more rapid decline of infected cells resulting in lower minima. This improved ability to eliminate infected cells is expected to come at the cost of higher pathology during acute infection as a result of the higher amount of virus that is present.

A methodological difficulty of this investigation was that the outcomes of the models could only be explored with numerical simulations. Therefore, the outcomes were investigated over wide ranges of each parameter. Only the patterns reported here were discovered. The choice of parameters in these models were not based on any particular infection, and we are not aware of what parameter values would be biologically realistic for the infections discussed here. Parameter measurement in the context of specific infections will be the next step in supporting the claim that a delayed CTL response can be adaptive.

Our model assumed a delay in the arrival of CTL at the site of infection, which was modelled by assuming that it takes a certain amount of time for differentiated effector CTL to migrate to the site of the infection. A similar effect would be observed if it was assumed that CTL only became activated once the virus load had crossed a certain threshold. Indeed, this explanation was invoked for a CTL delay in a kinetic analysis of HIV infection data in

the context of a vaccine trial (Davenport et al 2004). While the biological mechanism would be different, the net effect is similar.

As mentioned in the Introduction, a study conducted by Frey *et al.* examining the spatio-temporal dynamics of CTL responses against PVM provided the strongest evidence for a delayed arrival of CTL to the site of infection (Frey et al 2013). Indeed, this experimental study motivated our work with the aim to offer a possible explanation for these results. The CTL responses were observed to infiltrate the lung only after maximal virus load was achieved, and this coincided with the development of symptomatic pathology in the mice. The authors of this study speculated that these characteristics might enhance the ability of the CTL response to clear the infection. Using mathematical models, we provided a theoretical basis for this claim. The model suggests that allowing the virus to grow to near maximal levels might indeed enhance the ability of the CTL to clear the infection under certain conditions and via the following mechanisms: late CTL responses allow the virus to deplete its source of growth (the target cells), and higher virus loads cause resting CTL to be recruited at a higher rate. The model further suggests that there might be a general trade-off between the level of acute virus load/pathology and the ability of a CTL response to clear a virus infection. While responding early when the virus load is small will reduce the degree of pathology, it can reduce the chances to clear the infection in the long-term, which could be costly. A CTL delay can also result in pathology from the CTL themselves in that they perform their function by killing the hosts own cells. In light of the hypothesis driving this project, it can therefore be speculated that a delayed CTL response has evolved against other selection pressures in order to maximize the chances that the infection is successfully resolved.

In the context of vaccination, it is thought that delayed CTL responses to challenge present an obstacle to successful CTL-mediated protection against infection (De Boer, 2007; Wodarz et al. 2000). The goal of vaccination is often to increase the speed with which CTL arrive at the site of infection. Although this would be the best strategy to prevent infection in the first place, this immune response may have instead evolved to maximize the chances of virus clearance, which may explain some of the difficulties observed in the context of CTL-based vaccination approaches.

It is important to consider that, while under some parameter regimes a delayed CTL response can be more effective at clearing an infection, under others it is better for CTL to arrive at the site of the infection as soon as possible. Which outcome is observed depends on measures such as the replication rate of the virus and the rate of tissue turnover, which vary from one infection to another. This may lead one to speculate as to whether a universal CTL delay evolved, arising from the greater selection pressures of viruses more effectively cleared with a delay. This would of course imply that CTL responses to other infections are less effective than they could be. From an experimental point of view, it would be constructive to perform a comparative study of the spatio-temporal dynamics of different infections in different tissues. The work of this project suggests that a delay may or may not be beneficial to the host depending on the conditions, thus it will be important to measure crucial parameters such as the rate of tissue turnover and the replication rate of the virus. It would also be of interest as to whether different CTL delays exist for different infections and whether the amount of delay is adaptive in each case.

References

Asquith, B., McLean, A. R. 2007. In vivo CD8+ T cell control of immunodeficiency virus infection in humans and macaques. *Natl Acad Sci* 104:6365-6370.

Frey, S. Pricher, H., Follo, M., Collinsm P., Krempl, C., Ehl, S. 2002. In situ evolution of virus-specific cytotoxic T cell responses in the lung. *Proc Natl Acad Sci* 15:661-668.

Goulder, P. J., Watkins, D. I. 2004. HIV and SIV CTL escapte: implications for vaccine design. *Nat Rev Immunol* 630-640.

Guidotti, L. G, Chisari, F. V. 2006. Immunobiology and pathogenesis of viral hepatitis. *Annu Rev Pathol* 1:23-61.

Guidotti, L. G., Rochford, R., Chung, J., Shapiro, M., Purcell, R. 1999. Viral clearance without destruction of infected cells during acute HBV infection. *Science* 284:825-829.

Kundig, T. M. 1996. On the role of antigen in maintaining cytotoxic T-cell memory. *Proc Natl Acad Sci* 93:9716-9723.

Lechner F, et al. 2004. CD8 eptiope escape and reversion in acute HCV infection. *J Exp Med* 200:1593-1604.

Leslie, A. J. et al. 2004. HIV evolution: CTL escape mutation and reversion after transmission. *Nat Med* 10:282-289.

Levy, J. A., Machewicz, C. E., Barker, E. 1996. Controlling HIV pathogenesis: the role of the noncytotoxic anti-HIV response of CD8+ T cells. *Immunol Today* 17:217-224.

Maini, M. K. et al. 2000. The role of virus-specific CD8+ cells in liver damage and viral control during persistent hepatitis B virus infection. *J Exp Med* 191:1269-1280.

Moskohidis, D., Battergay, M, van den Broek, M., Laine, E., Hoffmann-Rohrer, U. Zinkernagel, R. M. 1995. Role of virus and host variables in virus persistence or immunopathologicla

disease caused by a non-cytolytic virus. *J Gen Virol* 76:381-391.

Nelson, D. R., Marousis, C. G., Davis, G. L., Rice, C. M., Wong, J. 1997. The role of hepatitis C virs-specific cytotoxic T lymphocutes in chronic hepatitis. *J Immunol* 158:1473-1481.

Novak, M. A., May, R. M. (2000) "Virus Dynamics. Mathematical Principles of Epidemiology and Virology." Oxford, UK: Oxford University Press.

Rowland-Jones, S., Tan, R., McMichael, A. 1997. Role of cellular immunity in protection against HIV infection. *Adv Immunol* 65:277-346.

Seich Al Basaten, N. K., Chatzimichalis, K., Graw, R., Frost, S. D, Rogoes, R. R., Asquith, B. 2013. Can non-lytic CD8+ T cells drive HIV-1 escape? *PLoS pathog* 9:31003656.

Sobao, Y. et al. 2002. The role of hepatitis B virus-specific memory CD8 T cells in the control of viral replication. *J Hepatol* 36:105-115.

Timm, J. et al. 2004. CD8 epitope excape and reverwsion in acute HCV infection. *J Exp Med* 200:1593-1604.

Zinkernagel, R. M., Hengartner, H. 1994. T-cell-mediated immunopathology versus direct cytolsysis by virus: implications for HIV and AIDs. *Immunol Today* 15:262-268.

Chapter 2: The role of mortality and cultural transmission in human fertility decline

2.1 Introduction

"Demographic transition" refers to a marked change in the demographic variables of a society, which can include measures of birth and death. The demographic transition of concern here is that of Europe and North America over the last few centuries and more recently in many developing countries. This transition is characterized by a radical decline in birth and death rates, with the latter often preceding the former (Kirk, 1996).

The mortality rate in pretransition societies is high (Livi-Bacci, 2017). In fact, it is even higher than that of the hunter-gatherer societies that preceded them. The most widely accepted explanation for the high mortality of this mode of life is the high population-density. Frequent contacts between humans and other animals increase the rate of infection. Poor nutrition from an unvaried diet might also be a contributor and could very well limit the population's ability to fight infection.

The decline of mortality in the early part of the European transition is notable, as it preceded improvements in sewage control that occurred in the 1870's and long before the availability and distribution of sulfonamides (McKeown, 1972; Bengtsson, 2001). Although the first smallpox vaccine had been developed, its impact could by no means account for the entirety of this mortality decline. One proposed explanation for this early decline relates to increases in food production that enabled the population to better resist infection, while another relates to improvements in personal hygiene, which include more frequent bathing and washing, use of soap, and the use of cotton clothing (Razzell, 1974).

Whatever the reason for this early decline in mortality, life expectancy gains in the 19th century were modest in comparison to those of the 20th century. While the population of Europe gained 10 years of life expectancy in the 1800's, it gained over 30 in the 1900s, and the evidence suggests that the bulk of this increase was due to the control and treatment of infectious disease (Preston, 1976).

Early theories concerning the fertility component of the demographic transition proposed that fertility declines were caused by the lifestyle and low mortality conditions that accompany economic development (Kirk, 1996; Notestein, 1945; Thomson, 1929). Low mortality resulted in larger families in the absence of fertility control. The economic benefit of children also declined as sources of production shifted away from the family to a larger scale, children were no longer available as sources of labor due to mass schooling, and changes in social life provided alternatives to large families. However, later studies showed only a minor correlation between fertility and socioeconomic variables and that regions that underwent a fertility transition often shared a similar language and culture (Knodel and Van de Walle, 1979). In response, scholars proposed "ideational" theories for fertility decline. In the case of Lesthaeghe (1983), a set of societal values emphasizing the individual were established, such that individuals now made decisions that resulted in lower fertility in a number of ways. For Cleland and Wilson (1987), this meant the establishment of social norms that promoted the access to, knowledge of, and the willingness to implement various means of birth reduction. Still later scholars disputed the claim that either of socioeconomic or ideational explanations should be favored, maintaining that families may still limit fertility according to their micro- and macro-economic circumstances in ways that have not been given attention by demographers

(Hirschman, 1994; Mason, 1997). This view allows for a complex interaction between societal values, i.e., ideation, economic conditions, and individual decision making. Such scholars also stressed the consideration of a causal role for mortality as in the classical theories of transition.

The demographic transition may at first seem counterintuitive in evolutionary terms, as human beings appear to be limiting their reproduction during times of apparently abundant resources. Although maximum levels of fertility may not be optimal in a variety of environmental conditions, the magnitude of the decline in fertility is striking and deserves an explanation. Furthermore, fertility is negatively correlated with wealth in post-transition societies, when the evidence suggests that the opposite is the case in pre-transition societies (Cronk, 1991; Perusse, 1993; Vining, 1986).

Various explanations for fertility reduction in humans have been proposed from an evolutionary perspective. One proposal is that humans may be making a quantity-quality tradeoff because of the high parental investment required of each child in modern societies. Unfortunately, this hypothesis has no empirical support, as it appears that men who have the most children also have the most grandchildren (Kaplan, 1995). Theory would predict that the number of grandchildren should peak at some intermediate level of fertility if this hypothesis were correct. Others have claimed that fertility reduction is simply a poor evolutionary adaptation to a radically different environment, particularly as a result of modern contraception. Although it has been shown that high status men in a Canadian sample copulated more frequently than low status men, which would result in more offspring in the absence of contraception (Perusse, 1993), this explanation does not stand up against the evidence of history and certain modern societies in the pre-transition phase.

The fertility decline in Europe began long before effective contraception was widely available (Knodell and van de Walle, 1979), and some African countries have yet to undergo a transition, despite the availability of contraception. Overall, the major weakness of the adaptive-lag hypothesis is that it does not specify what in the environment has changed and why this change results in a lower fertility.

There is now a vast literature on cultural evolution and transmission (Mesoudi, 2017; Creanza, 2017). Models of cultural transmission have been applied to the matter of fertility decline by groups led by Feldman (Cavalli-Sforza and Feldman, 1981; Fogarty et al., 2013; Ihara and Feldman, 2004). The simplest of these models is merely an infection model of the Lotka-Volterra form. Not surprisingly, when low-fertility individuals convert members of the high-fertility population at some rate, the low fertility population invades at sufficiently high rates of transmission. In a niche construction approach, two cultural traits are transmitted: one coding for a preference for some background trait (such as the tendency to prefer education), and the other for a tendency to have fewer offspring. It is assumed that there is a positive relationship between the frequency of the background trait and the rate of learning from non-parental adults. Provided that those with fewer offspring are overrepresented in transmission from non-parental adults, the low fertility trait can invade the population. When the frequency of the background trait is positively associated with the survival of individuals, the relative average fertility decreases following a decrease in mortality in a way similar to that observed in the demographic transition of the last two centuries. In a later model, fertility, mortality, and cultural transmission have an age-structure, such that reproduction and mortality vary throughout the lifespan of individuals, and individuals acquire a cultural trait at different rates depending on if the individual

learned from is a parent, same-age peer, or non-parental adult. In this model, when the cultural trait reduces fertility and increases survival, the age-structure of the population resembles that of Western societies after demographic transition, provided the rate of transmission from same-age peers and non-parental adults is high.

Although two of the above models include mortality explicitly, in one case mortality reduction spreads through a cultural trait that increases transmission, and in the other case mortality reduction is endogenous to the fertility-reducing trait itself. In the models that follow, mortality is considered as an exogenous variable, alongside parameters which vary the rate of transmission and the social status of low-fertility individuals. The following simulations model populations in which a fertility-reducing trait spreads via cultural transmission in both spatial and non-spatial settings, with and without age-structure.

2.2 One Age-Class

The results have been obtained using an agent-based model that employs birth and death processes combined with a voter model framework. Agents occupy a grid containing $n \times n$ spaces. Agents are one of two types: high-fertility (h) and low-fertility (l). The grid is sampled randomly 2m times, where m is the total number of individuals currently occupying the grid. Should a given sampling land on a space occupied by an individual, there is 0.50 probability that a birth/death procedure will be applied and a 0.50 probability that a voting procedure will be applied.

When the birth/death procedure is applied, the individual chosen reproduces with a probability $p_{repr}(h)$ or $p_{repr}(l)$, depending on whether the individual is of high- or low-

fertility, and dies with a probability p_{death}. If an individual reproduces, their offspring is placed randomly into one of the neighboring spaces on the grid. Reproduction does not take place if this space is already occupied. The offspring of an individual are of the same fertility type as their parent. When an individual dies, the space that they occupy becomes empty.

Individuals chosen to vote are converted to the opposite fertility type (high or low) with a probability equal to the frequency of this opposite type among their neighbors. The social status of high-fertility individuals is also adjustable by a parameter p_{comm}, such that they are not included in the voting procedure with a probability $1-p_{comm}$. Additionally, the influence of voting relative to reproduction and death can be modified by a parameter $p_{transmit}$, such that the voting procedure is skipped altogether with a probability $1-p_{transmit}$.

This framework is applied under two different assumptions regarding spatial interactions. First, we consider two competing populations who can only interact with their nearest-neighboring positions in both reproduction and voting mechanisms. When individuals reproduce, they can only place their offspring in a nearest-neighboring position if it is unoccupied. When individuals vote, they can only consider the fertility types of individuals in the nearest-neighboring positions. Second, we consider perfect mixing, such that individuals can place their offspring randomly into any unoccupied space on the grid, and the radius of individuals included in the voting procedure encompasses the entire grid. In section 2.4, we apply these same considerations to two competing age-structured populations. Non-periodic boundary conditions are assumed throughout.

2.3 i. Nearest-Neighbor Interactions

We first describe the basic mechanisms of the model independently of each other. When birth and death processes are at work in the absence of any voting procedure, one population excludes the other with some frequency that depends on the reproduction rate, common death rate, and the initial frequencies of both populations. The winning population grows according to common logistic growth dynamics.

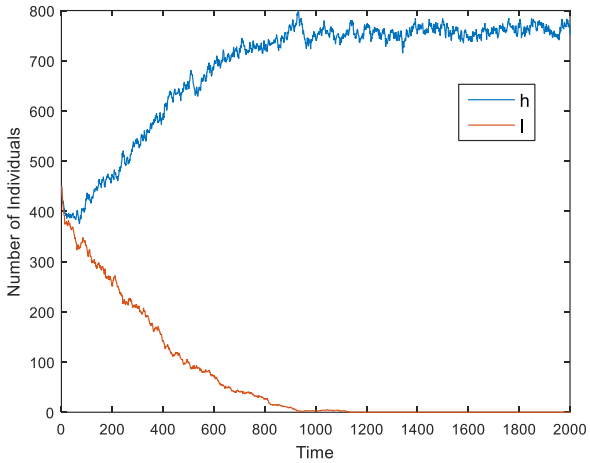

Fig. 1. Competing populations with only birth/death process. Initial number of both h (high fertility) and l (low fertility) individuals is 450. Reproduction probability of the high-fertility population: $p_{repr}(h) = 0.07$. Reproduction probability of the low-fertility population: $p_{repr}(l) = 0.05$. Common mortality rate: $p_{death} = 0.01$. Winning population displays common logistic growth dynamics.

One should note that the only long-term outcome of stochastic population models is the extinction of both populations. Additionally, both populations might persist long enough in such models as to imply coexistence in practical terms. However, in the parameter regimes given in Figs. 1 and 2, the competitive exclusion of one population to the other occurs at such short time scales that these qualifications are not relevant for our analysis.

We next consider the voter model dynamics in the absence of any reproduction and mortality (Fig. 3.). The designation of h or l represents arbitrary labeling in this scenario, except insofar as population h can be given lesser weight in the voting procedure by a parameter p_{comm}. In this case, when we start with a full grid, the outcome is entirely determined by drift dynamics, with the long-term outcome being that the whole population is of one type or the other (h or l).

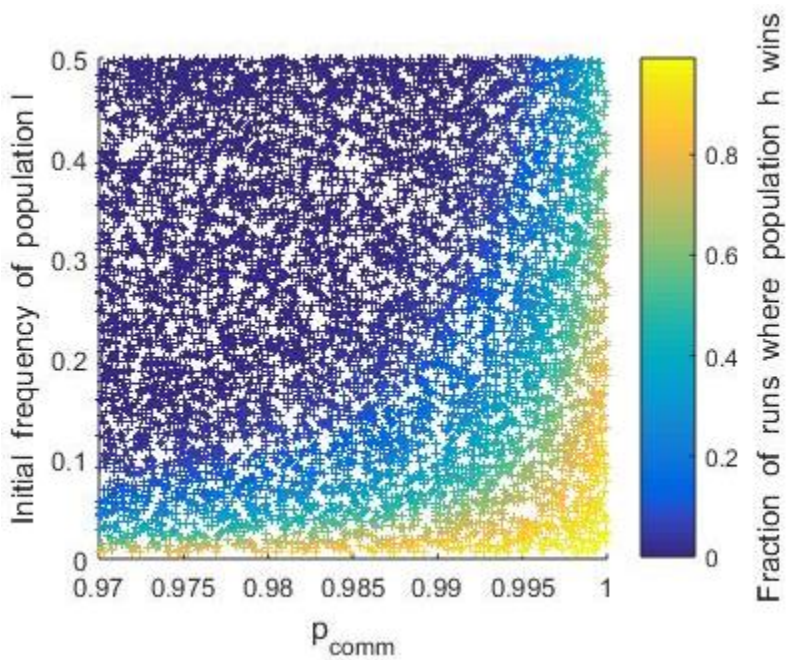

Fig. 2. Fraction of runs where population h wins in a voter model dynamic with respect to p_{comm} (the frequency with which population h is considered in the voting procedure) and the initial frequency of population l. n =30. The frequency of population h wins decreases as p_{comm} and the initial frequency of population l decrease. p_{comm} has a greater effect on the outcome than the initial frequency of population l. Each data point reflects the frequency of h wins out of 500 runs. 7396 data points.

When $p_{comm} = 1.00$ and the populations start at equal frequency, each population has an equal chance of fixation. The frequency of population l wins increases as its initial

frequency is increased and p_{comm} is decreased. p_{comm} has a far greater influence on the outcome than the initial composition of the population, as can be seen in the scale of the horizontal axis. Population h needs a considerable advantage in initial frequency in order to win at a low p_{comm}.

Now we combine these mechanisms and investigate the outcome for various values of p_{comm}, $p_{transmit}$, and p_{death}. We find that population l is more likely to invade or win at high values of $p_{transmit}$, low values of p_{comm}, and low values of p_{death} (Figs 3, 4, and 5). Unlike the outcomes observed when the mechanisms of birth/death and voting operate in isolation, some parameter regimes allow both populations to persist for a considerable amount of time, such that they coexist for all practical purposes. Thus, coexistence is defined arbitrarily as both populations coexisting for more than 100,000 time steps. This coexistence is obtained at intermediate values of the three parameters.

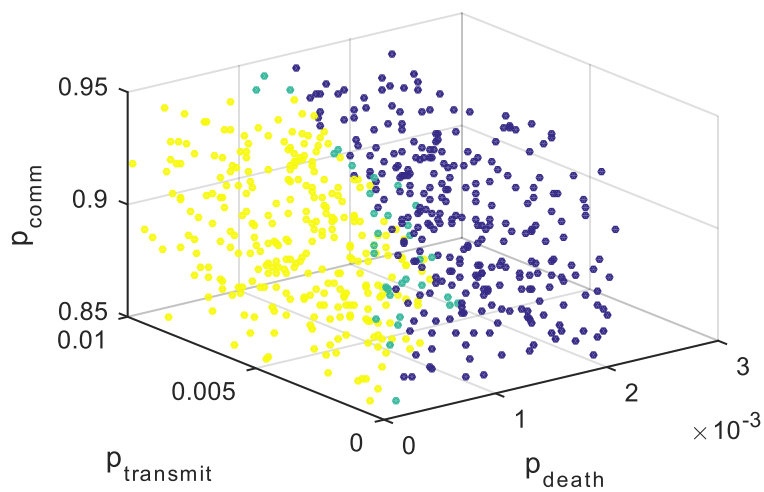

Fig. 3. Exclusion/coexistence outcomes of model with both voting and birth/death mechanisms. Nearest-neighbor interactions. Outcomes are shown with respect to the rate of voting ($p_{transmit}$), mortality (p_{death}), and the weight of high-fertility individuals in the voting procedure (p_{comm}). n = 30. Reproduction probability of population h (high fertility): p_{repr} (h) = 0.05. Reproduction probability of population l (low fertility): p_{repr}(l) = 0.03. Initial population of h individuals = 450. Initial population l individuals = 450. Purple: population h wins. Yellow: population l wins. Green: coexistence. 604 data points.

Population l wins with greater frequency as $p_{transmit}$ is increased and p_{comm} and p_{death} decrease. Coexistence is obtained for intermediate values of these variables.

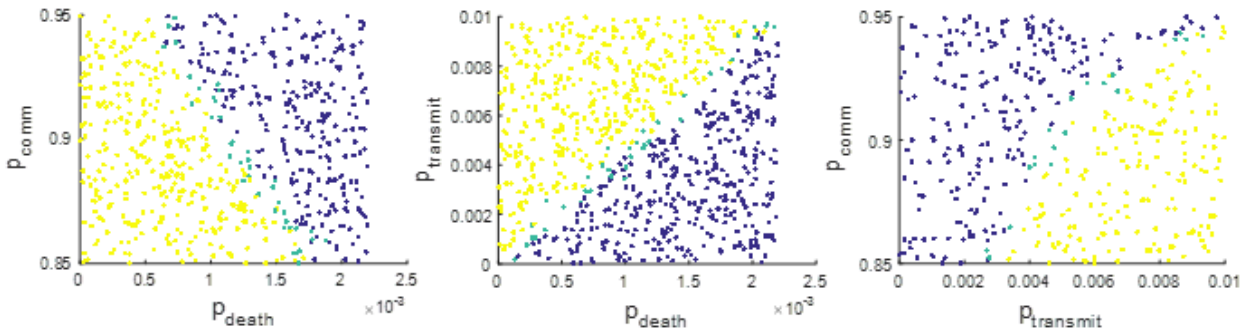

Fig.4. Cross-sections of Fig. 3. Purple: population h wins. Yellow: population l wins. Green: coexistence. Left: Outcome with respect to p_{comm} and p_{death}. Population l is more likely to win as p_{comm} and p_{death} are lowered. 625 data points. Center: Outcome with respect to $p_{transmit}$ and p_{death}. Population l is more likely to win as p_{death} is lowered and $p_{transmit}$ is increased. 625 data points. Right: Outcome with respect to p_{comm} and $p_{transmit}$. Population l is more likely to win as p_{comm} is decreased and $p_{transmit}$ is increased. 410 data points.

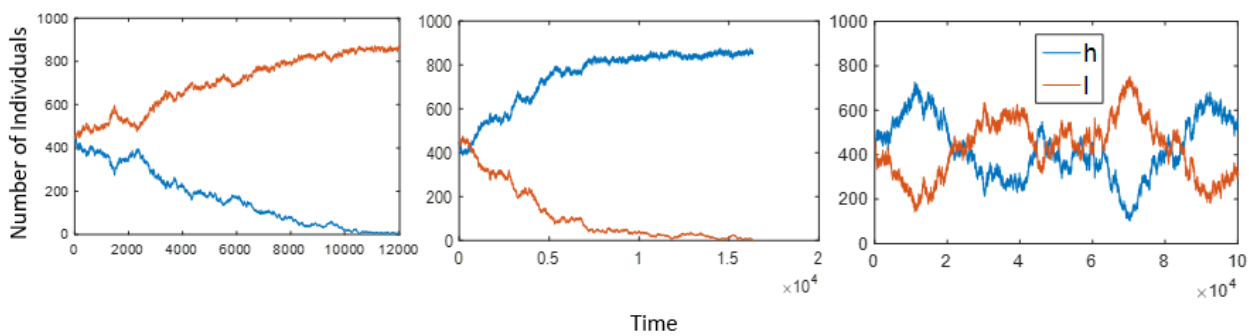

Fig. 5. Time series of three possible outcomes of model with both voting and birth/death mechanisms. Nearest-neighbor interactions. Reproduction probability of population h (high fertility): p_{repr} (h) = 0.05. Reproduction probability of population l (low fertility): p_{repr}(l) = 0.03. Left: Population l wins. p_{death}=0.00102; $p_{transmit}$= 0.00810; p_{comm}= 0.88865. Center: Population h wins. p_{death}=0.00181; $p_{transmit}$= 0.00402; p_{comm}= 0.87607. Right: Coexistence between populations h and l. p_{death}=0.00185; $p_{transmit}$= 0.00594; p_{comm}= 0.86714.

2.3 ii. Perfect Mixing

In this scenario, we investigate the outcomes of the same model under the assumption of perfect mixing. Rather than limiting individuals to their nearest-neighboring positions, individuals can place their offspring into any unoccupied space on the grid, and the radius of individuals considered in the voting procedure encompasses the entire grid. Such assumptions will also allow us to represent the model as a system of ordinary differential equations.

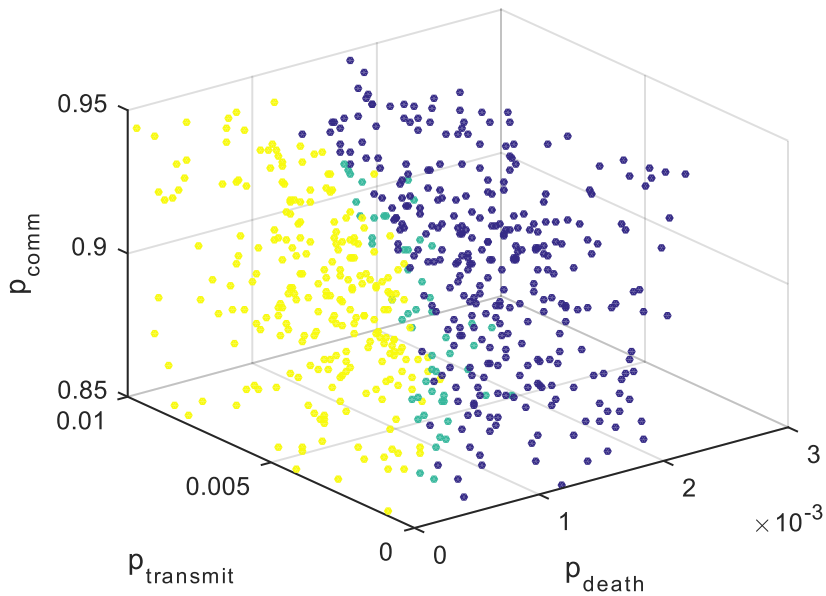

Fig. 6. Exclusion/coexistence outcomes of model with both voting and birth/death mechanisms. Perfect mixing. Outcomes are shown with respect to the rate of cultural transmission ($p_{transmit}$), mortality (p_{death}), and the weight of high-fertility individuals in the voting procedure (p_{comm}). n = 30. Reproduction probability of population h (high fertility): $p_{repr}(h) = 0.05$. Reproduction probability of population l (low fertility): $p_{repr}(l) = 0.03$. Initial population of h individuals = 450. Initial population of l individuals = 450. Purple: population h wins. Yellow: population l wins. Green: coexistence. 604 data points. Population l wins with greater frequency as $p_{transmit}$ is increased and p_{comm} and p_{death} are decreased. Coexistence is obtained for intermediate values of these variables.

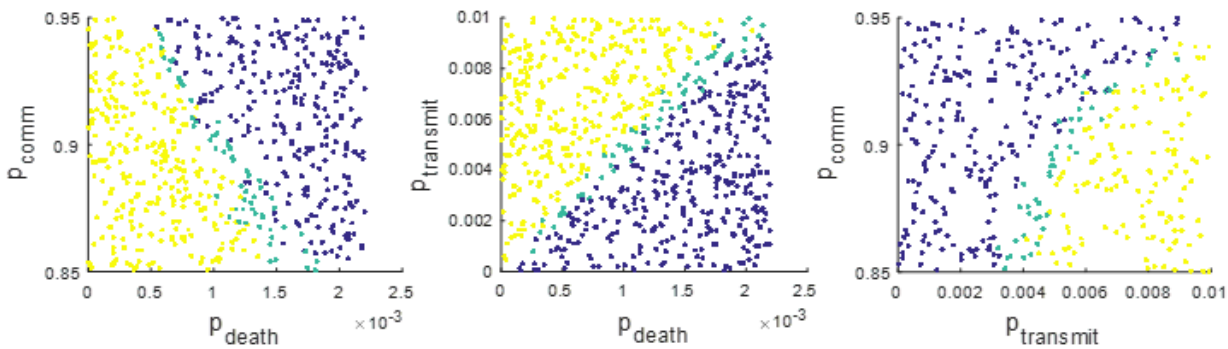

Fig. 7. Cross-sections of Fig. 6. Purple: population h wins. Yellow: population l wins. Green: coexistence. Left: Outcome with respect to p_{comm} and p_{death}. Population l is more likely to win as p_{comm} and p_{death} are lowered. 407 data points. Center: Outcome with respect to $p_{transmit}$ and p_{death}. Population l is more likely to win as p_{death} is lowered and $p_{transmit}$ is increased. 783 data points. Right: Outcome with respect to p_{comm} and $p_{transmit}$. Population l is more likely to win as p_{comm} is decreased and $p_{transmit}$ is increased. 410 data points.

Comparable results were achieved to those in the nearest-neighbors scenario, with the additional artifact that coexistence occurs more frequently and over a wider parameter regime (Figs 6 and 7). (Comparable time series are obtained as for the model with nearest-neighbor interactions, as well as for remaining models, thus they are not shown.) Population l is more likely to invade or become fixed at high values of $p_{transmit}$, low values of p_{comm}, and low values of p_{death}.

The ordinary differential equations that describe the dynamics are as follows.

$$\dot{x}_h = r_h x_h \left(1 - \frac{x_h + x_l}{K}\right) - d x_h - \frac{\beta_l x_h x_l}{x_h + x_l} + \frac{\beta_h x_h x_l}{x_h + x_l}$$

$$\dot{x}_l = r_l x_l \left(1 - \frac{x_h + x_l}{K}\right) - d x_l + \frac{\beta_l x_h x_l}{x_h + x_l} - \frac{\beta_h x_h x_l}{x_h + x_l}$$

Representing the model this way allows one to determine possible equilibria and the conditions for their stability analytically. x_h and x_l give the numbers of high- and low-

fertility individuals, respectively. r_h and r_l give the intrinsic rates of increase of populations h and l, where $r_h > r_l$ to reflect the higher fertility of population h, and K represents the density-dependence of growth. The populations share a common death rate d. Individuals of each population are converted to members of the other population at a rate proportional to the frequency of the other type multiplied by a rate constant β_h or β_l. If we assume that population l is more effective at conversion than population h, such that $\beta_l > \beta_h$, and allow $\beta = \beta_l - \beta_h$, the system simplifies to

$$\dot{x}_h = r_h x_h \left(1 - \frac{x_h + x_l}{K}\right) - d x_h - \frac{\beta x_h x_l}{x_h + x_l}$$

$$\dot{x}_l = r_l x_l \left(1 - \frac{x_h + x_l}{K}\right) - d x_l + \frac{\beta x_h x_l}{x_h + x_l}$$

The resulting system is an infection model with density-dependent infection terms. The density-dependence of conversion is not relevant for our analysis, so these terms can be dropped, rendering

$$\dot{x}_h = r_h x_h \left(1 - \frac{x_h + x_l}{K}\right) - d x_h - \beta x_h x_l$$

$$\dot{x}_l = r_l x_l \left(1 - \frac{x_h + x_l}{K}\right) - d x_l + \beta x_h x_l$$

The system can converge to the following equilibria.

$x_h^{(0)} = 0$

$x_l^{(0)} = 0$

(Trivial equilibrium. Both populations go extinct.)

$x_h^{(1)} = \frac{K(r_h - d)}{r_h}$

$x_l^{(1)} = 0$

(High-fertility excludes low-fertility population)

$x_h^{(2)} = 0$

$x_l^{(2)} = \frac{K(r_l - d)}{r_l}$

(Low-fertility excludes high-fertility population.)

$x_h^{(3)} = \frac{\beta dK + dr_h - dr_l - \beta K r_l}{\beta(\beta K + r_h - r_l)}$

$x_l^{(3)} = \frac{\beta dr_h + dr_h - dr_l - \beta dK}{\beta(\beta K + r_h - r_l)}$

(High- and low-fertility populations coexist.)

The trivial equilibrium is stable when $r_h < d$ and $r_l < d$. Population h wins when

$$d > \frac{\beta K r_h}{\beta K + r_h - r_l}$$

Population l wins if

$$\frac{\beta K r_l}{\beta K + r_h - r_l} > d$$

Mathematica shows that the system has no bistability when the trivial equilibrium is not obtained, thus coexistence is obtained when

$$\frac{\beta K r_h}{\beta K + r_h - r_l} > d > \frac{\beta K r_l}{\beta K + r_h - r_l}$$

and the conditions for the trivial equilibrium do not hold.

The behavior of the system can also be assessed in terms of the basic reproductive ratio, R_0, a measure in infectious disease dynamics which gives the average number of infected agents that arise in the lifetime of a single infectious agent when placed into a completely uninfected population. An infection becomes established in a population when $R_0 > 1$. R_0 can be derived for the above infection model by determining the conditions under which the growth rate of population l is positive at very low numbers, when the system consists almost entirely of h individuals. This method renders the following value for R_0:

$$\frac{\beta K r_h}{d(r_l - r_h + \beta K)}$$

Thus, population l will invade when the above expression exceeds 1.

2.4 Four Age-Classes

We now consider the same framework with four age-classes instead of one. This allows us to vary an individual's fertility depending on its age. Individuals remain in each age-class for 100 time-steps before advancing to the next. Neither population h nor l reproduces in the first or last age-class, which represent the pre- and post-reproductive stages of life, respectively. Population h begins reproduction in the second age-class; population l begins reproduction in the third age-class. Populations h and l have the same rate of reproduction in the third age class. Mortality is held constant across age-classes, as our main interest lies in the conditions under which a population with a delayed reproduction can outcompete a population which begins reproduction earlier in life. All individuals die after spending 100 time steps in the 4th age-class.

As before, individuals occupy an $n \times n$ grid, and the grid is sampled 2m times, where m is the number of individuals currently occupying the grid. For each sampling there is a 0.50 probability that the birth/death routine will be applied and 0.50 probability that the voting routine will be applied. When the birth/death routine is chosen, individuals have a $p_{repr}(h_i)$ or $p_{repr}(l_i)$ probability of reproducing, depending on whether the individual is a member of population h or l, where i gives the age-class of the individual reproducing. i varies from 1 to 4. Individuals die with a probability p_{death}, which does not depend on age-class or whether the individual belongs to the h or l population. The voting routine functions the same as in the previous model and does not depend on the age-class of the individual that is voting or the surrounding individuals that are considered in the voting

procedure. Nearest-neighbor interactions and complete mixing are investigated separately as in the previous section.

2.4 i. Nearest-Neighbor Interactions

Comparable results were observed as for those of a single age-class (Figs 8 and 9). Population l is more likely to win at high values of $p_{transmit}$ and low values of p_{comm} and p_{death}. Coexistence is achieved at intermediate parameter values. This outcome is defined as both populations persisting together for more than 100,000 time steps.

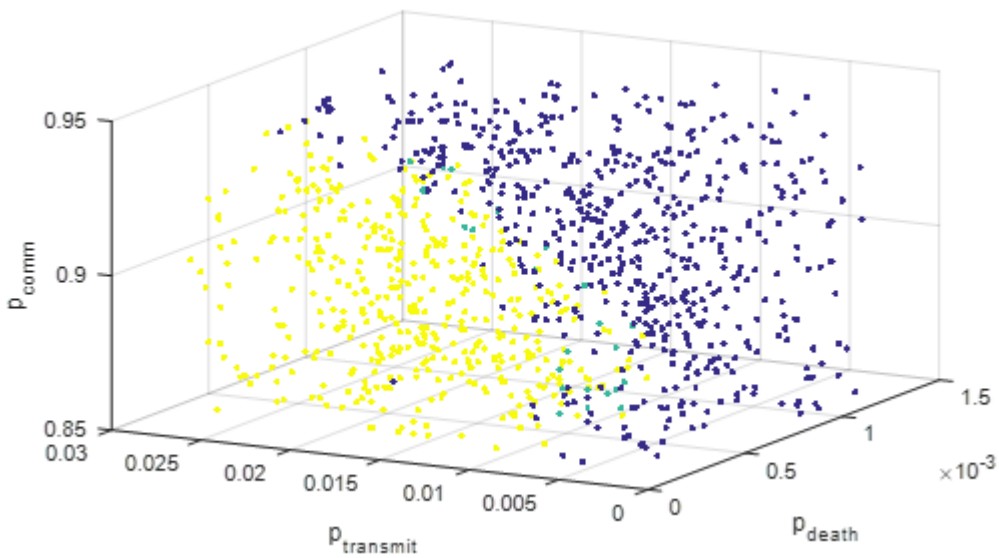

Fig. 8. Exclusion/coexistence outcomes of age-structured model with voting and birth/death processes. Nearest-neighbor interactions. Outcomes are shown with respect to the rate of cultural transmission ($p_{transmit}$), mortality (p_{death}), and the weight of high-fertility individuals in the voting procedure (p_{comm}). n = 30. Reproduction probabilities of successive age-classes of population h (high fertility) are as follows: $p_{repr}(h_1) = 0.0$; $p_{repr}(h_2) = 0.3333$; $p_{repr}(h_3) = 0.3333$; $p_{repr}(h_4) = 0.0$. Reproduction probabilities of successive age-classes of population l (low fertility) are as follows: $p_{repr}(l_1) = 0.0$; $p_{repr}(l_2) = 0.0$; $p_{repr}(l_3) = 0.03333$; $p_{repr}(l_4) = 0.0$. Initial population of h individuals = 450. Initial population l individuals = 450. Purple: population h wins. Yellow: population l wins. Green:

coexistence. Population l wins with greater frequency as $p_{transmit}$ is increased and p_{comm} and p_{death} are decreased. Coexistence is obtained for intermediate values of these variables. 600 data points.

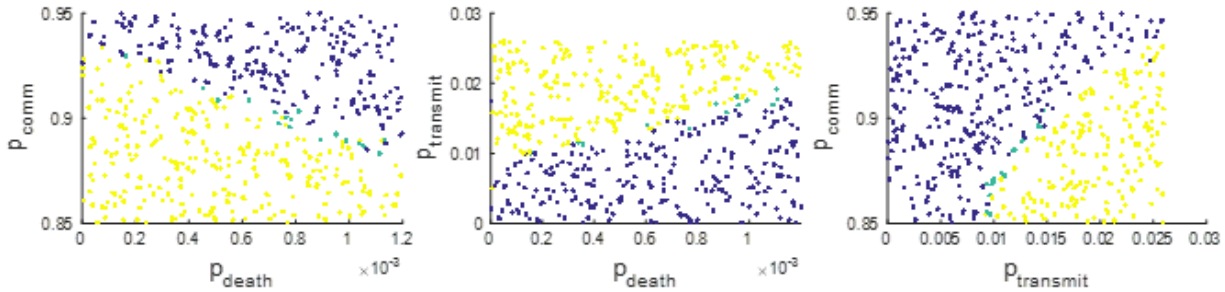

Fig. 9. Cross-sections of Fig. 8. Purple: population h wins. Yellow: population l wins. Green: coexistence. Left: Outcome with respect to p_{comm} and p_{death}. Population l is more likely to win as p_{comm} and p_{death} are lowered. 500 data points. Center: Outcome with respect to $p_{transmit}$ and p_{death}. Population l is more likely to win as p_{death} is lowered and $p_{transmit}$ is increased. 500 data points. Right: Outcome with respect to p_{comm} and $p_{transmit}$. Population l is more likely to win as p_{comm} is decreased and $p_{transmit}$ is increased. 500 data points.

2.4 ii. Perfect Mixing

We now consider the outcomes and analysis of the age-structured model with perfect mixing. Outcomes comparable to the previous models were observed, and coexistence was more frequent with perfect-mixing than it was with nearest-neighbor interactions as was observed in the one-age-class model (Figs 10 & 11).

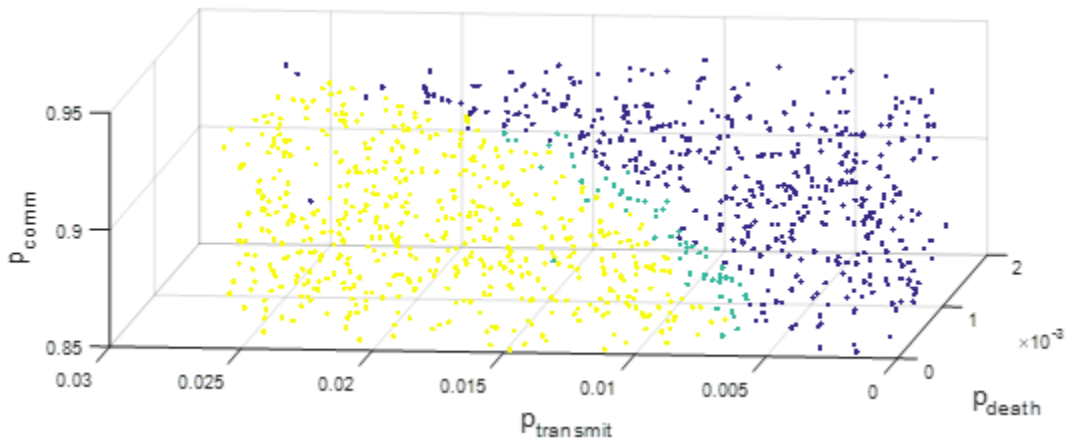

Fig. 10. Exclusion/coexistence outcomes of age-structured model with voting and birth/death processes. Perfect mixing. Outcomes are shown with respect to the rate of cultural transmission ($p_{transmit}$), mortality (p_{death}), and the weight of high-fertility individuals in the voting procedure (p_{comm}). n = 30. Reproduction probabilities of successive age-classes of population h (high fertility) are as follows: $p_{repr}(h_1) = 0.0$; $p_{repr}(h_2) = 0.3333$; $p_{repr}(h_3) = 0.3333$; $p_{repr}(h_4) = 0.0$. Reproduction probabilities of successive age-classes of population l (low fertility) are as follows: $p_{repr}(l_1) = 0.0$; $p_{repr}(l_2) = 0.0$; $p_{repr}(l_3) = 0.03333$; $p_{repr}(l_4) = 0.0$. Initial population of h individuals = 450. Initial population l individuals = 450. Purple: population h wins. Yellow: population l wins. Green: coexistence. Population l wins with greater frequency as $p_{transmit}$ is increased and p_{comm} and p_{death} are decreased. Coexistence is obtained for intermediate values of these variables. 1000 data points.

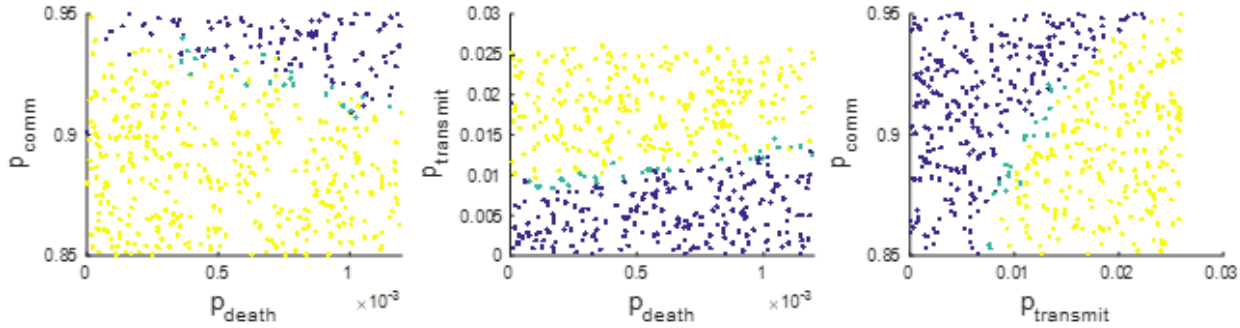

Fig. 11. Cross-sections of Fig. 10. Purple: population h wins. Yellow: population l wins. Green: coexistence. Left: Outcome with respect to p_{comm} and p_{death} . Population l is more likely to win as p_{comm} and p_{death} are lowered. 500 data points. Center: Outcome with respect to $p_{transmit}$ and p_{death}. Population l is more likely to win as p_{death} is lowered and $p_{transmit}$ is increased. 500 data points. Right: Outcome with respect to p_{comm} and $p_{transmit}$. Population l is more likely to win as p_{comm} is decreased and $p_{transmit}$ is increased. 500 data points

As with the one-age-class model, perfect mixing allows one to represent the model as a system of equations. Age-structured models are easily represented with systems of difference equations.

$$x_{1,t+1} = \frac{f_{x_1}}{q} x_{1,t} + \frac{f_{x_2}}{q} x_{2,t} + \frac{f_{x_3}}{q} x_{3,t} + \frac{f_{x_4}}{q} x_{4,t}$$

$$x_{2,t+1} = s_{x_1} x_{1,t} - s_{x_1} \beta_{xy} x_{1,t}$$

$$x_{3,t+1} = s_{x_2} x_{2,t} - s_{x_2} \beta_{xy} x_{2,t}$$

$$x_{4,t+1} = s_{x_3} x_{3,t} - s_{x_3} \beta_{xy} x_{3,t}$$

$$y_{1,t+1} = \frac{f_{y_1}}{q} y_{1,t} + \frac{f_{y_2}}{q} y_{2,t} + \frac{f_{y_3}}{q} y_{3,t} + \frac{f_{y_4}}{q} y_{4,t}$$

$$y_{2,t+1} = s_{y_1} y_{1,t} + s_{x_1} \beta_{xy} x_{1,t}$$

$$y_{3,t+1} = s_{y_2} y_{2,t} + s_{x_2} \beta_{xy} x_{2,t}$$

$$y_{4,t+1} = s_{y_3} y_{3,t} + s_{x_3} \beta_{xy} x_{3,t}$$

$x_{i,j}$ and $y_{i,j}$ represent the populations of high- and low-fertility individuals, respectively, at age-class i and time j. The f's represent the age-specific fertilities of x or y at the age-class given by the subscript of the variable, and q represents the density-dependence of fertility, which is given by

$$q = 1 + \frac{\sum_{i=1}^{4} x_{it} + \sum_{i=1}^{4} y_{it}}{N}$$

Density-dependence increases as N decreases. The s's represent the age-specific rates of survival from one age-class to the next and can be understood as the compliment of the

age-specific mortality rate. β_{xy} gives the net rate of conversion of high-fertility individuals to low-fertility individuals and is given by

$$\beta \times \frac{\sum_{i=1}^{4} y_{n,t}}{\sum_{i=1}^{4} x_{n,t} + \sum_{i=1}^{4} y_{n,t}},$$

where $0 \leq \beta \leq 1$ is a parameter which reflects the extent to which the rate of conversion increases with the frequency of y. The dynamics of this system are difficult to assess analytically. However, numerical simulations show that it is easier for the low-fertility population to invade as survival increases (or rather, as mortality decreases)(Fig. 12). The cycles seen in the low-fertility population of Fig. 12 d) are a common occurrence in populations with only one reproductive age-class. In such a case, a single cohort reproduces at only one age as it progresses through its life, at which point the population surges. When the original cohort dies, the offspring of this cohort constitute the only members of the population, and they are found in only one age-class. The cycle then repeats. Such cycling behavior is not observed in cases where both populations coexist, as age-classes 2-4 of the low-fertility population become filled when members of the high-fertility population are converted. This mechanism is evidenced by the fact that cycles of the low-fertility population in d) only appear when the high-fertility population begins to fall off at a much higher rate, at which point the rate of conversion of the high-fertility population is no longer sufficiently high to fill the age-classes of the low-fertility population.

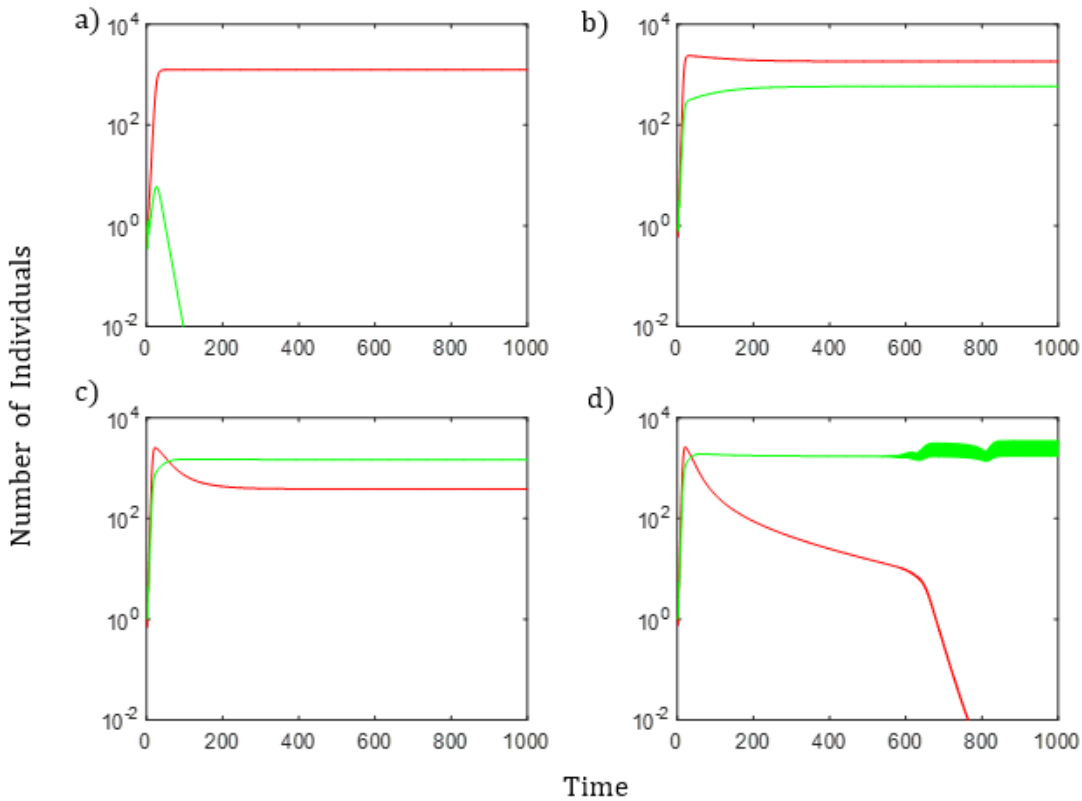

Fig. 12. Dynamics of competing age-structured populations as represented by difference equations. Members of the high-fertility population are converted to members of the low-fertility population at a rate proportional to the frequency of the low-fertility population. Green: Low-fertility population. Red: High-fertility population. All parameters but the age-specific rates of survival are held constant for each simulation. The age-specific fertilities of the high-fertility population are as follows: $f_{x1} = 0$, $f_{x2} = 3.0$, $f_{x3} = 3.0$, $f_{x4} = 0$. The age-specific fertilities of the low-fertility population are as follows: $f_{y1} = 0$; $f_{y2} = 0$; $f_{y3} = 3.0$; $f_{y4} = 0$. Fertility saturation term: $N = 1000$. Rate of conversion: $\beta = 0.40$. Age-specific survival rates are increased from a-d. a) $s_{x1} = s_{x2} = s_{x3} = s_{y1} = s_{y2} = s_{y3} = 0.50$. b) $s_{x1} = s_{x2} = s_{x3} = s_{y1} = s_{y2} = s_{y3} = 0.75$. c) $s_{x1} = s_{x2} = s_{x3} = s_{y1} = s_{y2} = s_{y3} = 0.875$. d) $s_{x1} = s_{x2} = s_{x3} = s_{y1} = s_{y2} = s_{y3} = 0.95$. The low-fertility population invades or becomes fixed as survival is increased.

2.5 Discussion

This chapter investigated the evolutionary dynamics of a fertility-reducing trait that is transmitted via a voter model framework in a reproducing population. The outcomes were investigated at varying rates of mortality and transmission and for varying weights of high-

fertility individuals in the voting routine. It was found that low-fertility individuals could persist in the population when the mortality rate and the weight of high-fertility individuals were low and the rate of cultural transmission was high. The basic framework was applied under conditions of nearest-neighbor interactions and perfect mixing, with and without age-structure with the same basic result.

Empirical data suggest that fertility transitions are difficult to initiate unless mortality is lowered first (Mason, 1997). The numerical and analytical results achieved via these simulations may provide some insight into a possible mechanism behind this observation. When viewed in the context of infection models, decreasing the mortality rate increases the population density, which in turn gives an advantage to the transmission process by increasing the frequency of contacts between individuals. In other words, lowering mortality increases the basic reproductive ratio of the infection (Heesterbeek, 2002). This connection between fertility reduction and density-dependence is consonant with data suggesting that birth rates in human populations have an inverse relationship with population density (Lutz, 2006).

Fertility transitions have occurred in Europe in regions which are very dissimilar in socioeconomic terms but share a common culture and language (Knodel and van de Walle, 1979). Conversely, bordering regions which are similar in terms of socioeconomic variables may not all undergo a fertility decline when they have different languages and culture. These patterns appear suggestive of a transmission process like that modelled in this project. This project considered both scenarios where cultural transmission operates under nearest-neighbor interactions and perfect mixing. Either assumption may be justified depending on the type of communication networks available. Under conditions of

perfect mixing, the breadth of the coexistence regime increased, which may have implications for the role of mass media and communications in the spread of this trait.

This chapter also compliments the work of Feldman et al. (1981; 2004; 2013), which did not consider mortality as an exogenous variable. The models share a finding of Feldman's work in that low-fertility individuals must be given greater weight in the transmission process in order to invade. This finding is consistent with the empirical observation that it is often social elites who adopt fertility reduction first (Cleland and Wilson, 1987; Knodel and van de Walle, 1979), and that individuals often imitate the behavior of others who have higher social status, even when this behavior has no obvious connection to social status (Henrich, 2001; Henrich and Gil-White, 2001).

One limitation of the model thus far is that it corresponds to the spread of a discrete trait when a continuum of fertilities is possible. Although investigating a discrete trait is convenient in deriving mechanisms analytically, a framework allowing for a continuum of traits deserves to be described. In addition, the model does not specify how social status is built or explain the inverse relationship between social status and fertility. This is to be addressed in the next chapter.

References

Bengtsson, Tommy. 2015. "Mortality: The great historical decline," *Pp. 868-873 in* James D. Wright *(ed.), International Encyclopedia of the Social & Behavioral Sciences*, 2nd edition, *vol.* 15. Amsterdam: *Elsevier.*

Cavalli-Sforza, L. L., Feldman, M. W. 1981. "Cultural Transmission and Evolution: A Quantitative Approach." Princeton: Princeton University Press.

Cleland, J., Wilson, C. 1987. Demand theories of the fertility transition: an iconoclastic view. Population Studies 41(1):5-30

Creanza, N., Kolodny, O., Feldman, M. W. 2017. Cultural evolutionary theory: how culture evolves and why it matters. PNAS 114(30):7782-7789

Cronk, L. 1991. Wealth, status and reproductive success among the Mukogodo. Am Anthropol 93:345-360

Fogarty, L., Creanza, N., Feldman, M. W. 2013. The role of cultural transmission in human demographic change: an age-structured model. Theor Pop Biol 88:68-77

Heesterbeek, J. A. 2002. A brief history of R_0 and a recipe for its calculation. Acta Biotheor 50:189-204

Henrich, J. 2008. Cultural transmission and the diffusion of innovations: adoption dynamics indicate that biased cultural transmission is the predominate force in behavioral change. Am. Anthrop. 103(4):992-1013

Henrich, J., Gil-White, F. 2001. The evolution of prestige. Evol and Hum Behav 22(3):165-196

Hirschman, C. 1994. Why fertility changes. Annu Rev Sociol 20:203-233

Ihara, Y., Feldman, M. W. 2004. Cultural niche construction and the evolution of small family size. Theor Pop Biol 65:105-111.

Kaplan, H. S. et al. 1995. Fertility and fitness among Albuquerque men: a competitive labour market theory, pp. 96-136 in "Human Reproductive Decisions." (Dunbar, R.I.M., ed.) St. Martin's Press.

Kirk, D. 1996. Demographic transition theory. Pop Stud 50(3):361-387

Knodel, J., van de Walle, E. 1979. Lessons from the past: policy implications of historical fertility studies. Popul and Devel Rev 5(2):217-245

Livi-Bacci, M. (2017). "A Concise History of World Population." Pp. 33-42. New Jersey: Wiley/Blackwell.

Lesthaeghe, R. A. 1983. A century of demographic and cultural change in Western Europe: an exploration of underlying dimensions. Popul Dev Rev 9:411-435

Lutz, W., Testa, M. R., Penn, D. J. 2006. Population density is a key factor in declining human fertility. Popul Environ 28:69-81

Mason, K. O. 1997. Explaining fertility transitions. Demography 34(4):443-454

McKeown, T, Brown, R. G., Record, R. G. 1972. An interpretation of the modern rise of population in Europe. Pop Stud 26(3):345-382

Mesoudi, A. 2017. Pursuing Darwin's curious parallel: Prospects for a science of cultural evolution. PNAS 114(30):7853-7860

Notestein, Frank W. (1945) "Population – the long view." Pp. 36-57 in T.W. Schultz. ed. Food for the World. Chicago: University of Chicago Press.

Perusse, D. 1993. Cultural and reproductive success in industrial societies: testing relationship at the proximate and ultimate levels. Behav Brain Sci 16:267-322

Preston, S. (1976). "Mortality Patterns in National Populations." Ch. 4. New York: Academic Press.

Razzell, P. 1974. An interpretation of a modern rise of population in Europe: a critique. Pop Stud 28(1):5-17

Thompson, W. 1929. Population. Am Journ of Sociol 34:959–75

Vining, D. R. 1986. Social versus reproductive success—the central theoretical problem of human sociobiology. Behav Brain Sci 9:167-260

Chapter 3: A continuous model of human fertility decline

3.1 Introduction

Many countries have undergone a reduction in fertility over the last few centuries (Kirk, 1996). Western European countries have in fact seen below replacement fertility since the 1970's and 1980's (Castles and Francis, 2003; Golstein et al. 2003). Classical theories of the demographic transition explained this fertility reduction in terms of changes in lifestyle that accompanied economic development (Notestein, 1945; Thompson, 1929). Mortality was much lower in developed countries, which would result in more children in the absence of fertility control; work in urban areas reduced economic incentives for large families; and mass schooling reduced the availability of children as sources of labor. Changes in social life also provided alternatives to large families. However, later studies showed only a modest correlation between fertility and measures of development (Knodel, 1979). Instead, it was shown that regions which underwent a fertility reduction shared similar languages and culture. Scholars then proposed ideational theories of fertility reduction, which relied on changes of values and social norms (Lesthaeghe, 1983; Cleland and Wilson 1987). As varied as theories of fertility reduction are, it is generally agreed that the fertility transition is difficult to initiate in the absence of a reduction in mortality (Mason, 1997).

It has been said that fertility reduction in the presence of abundant resources is the ultimate challenge to the application of evolutionary thinking to human behavior (Vining, 1986). This view could very easily be dismissed as shallow. Maximal reproduction

frequently does not maximize fitness. Organisms must weigh current reproduction against their offspring's survival and reproduction, the survival and reproduction of future generations, and their own future survival and reproduction. Such quantity-quality tradeoffs have been observed in African agricultural societies and, to some extent, hunter-gatherer societies (Lawson and Mace, 2011; Borgerhoff Mulder, 1997). However, studies of developed populations show no evidence of a quantity-quality tradeoff that results in greater long-term fitness (Kaplan et al. 1995; Kaptijn et al. 2010). Moreover, the upper classes tend to have fewer children than the lower classes, while their mortality rates are nearly the same. Clearly the higher fertility of lower classes is not a compensation for mortality which the upper classes lack.

The issue of fertility reduction is frequently discussed in terms of how fertility is related to social status. In the context of heritable wealth, it has been shown that when individual earning potential is low, long-term fitness is maximized when the wealth inherited by each offspring is high, which necessarily requires a lower rate of immediate reproduction (Rogers, 1990). In addition, low fertility appears to be fitness optimizing when the amount of resources invested in an individual offspring significantly increases the further resource generating ability of this offspring's lineage (Hill and Reeve, 2005). Other work on fertility with respect to social status advances the adaptive lag hypothesis—the claim that behaviors which previously maximized fitness among our ancestors are no longer operating to this end in the modern environment (Alvergne and Lummaa, 2014; Perusse, 1993). Fertility reduction operating via social status has also been captured in models of cultural transmission (Cavalli-Sforza and Feldman, 1981; Fogarty et al., 2013; Ihara and Feldman, 2004). In a cultural niche construction model, Ihara and Feldman

incorporated social status into their framework in the form of a preference for education. In this model, a preference for education serves as a culturally transmitted background trait, and this background trait is statistically associated with a fertility-reducing preference that is also culturally transmitted. The model shows that it is much easier for the fertility-reducing trait to invade when those with a preference for education are overrepresented in the transmission process.

Fertility often increases with social status in pretransition societies (Martin Fieder et al. 2005; Borgerhoff Mulder, 1988; Chagnon, 1988; Perusse, 1993). This fact makes sense for a social species. However, the opposite appears to be true in post-transition populations as a whole. One reason for this inverse relationship could be that, in modern societies, a higher social status requires extended periods of education and vocational training, both of which are not easily accrued while investing time and resources in dependent children. This claim is evidenced by the fact that education has always been inversely related to fertility for human civilization as a whole, whereas the relationship between status via income and occupation merely ceases to be strongly positive over historical time (Skirbekk 2008). One can increase income without investing in additional time-consuming training, but one cannot advance their education without some cost in terms of time. It has also been shown that for men, via mate selection, income is often positively related to fertility but education does not show a positive relationship as often (Fieder and Hubar, 2007; Hopcroft, 2015). The relationship between education and fertility is almost invariably negative for women, who invest more time in the care of their children and with extended education may miss their fertility window altogether (Huber et al. 2010; Fieder et al 2005).

Finally, simulations suggest that it is in fact fertility that impacts education more than the converse (Cohen et al 2011).

In the models that follow, the work of the previous chapter is supplemented by modelling the cultural transmission of a continuous trait. In the first set of models, social status is assumed to be endogenous to one's level of fertility, and individuals of low fertility are copied preferentially over individuals of higher fertility, with copying error. In the second set of models, an individual's social status is built gradually, but social status accrual is suspended for some time after the individual reproduces. Other members of the population copy the fertility rates of their neighbors according to the social status of these neighbors. Individuals are copied with error as before.

3.2 Results

Here, we model the cultural transmission of fertility in such a way that a continuum of fertilities can occur in the population. This is in contrast to the previous models, which only allowed for the possibility of two fertility types (high verses low). We accomplish this with two agent-based models which will be called ABM I and ABM II. The simulations differ in their assumptions about social status. In ABM I, individuals with a lower fertility are preferentially copied, thus an individual's social status is considered endogenous to their fertility. In ABM II, individuals build social status stochastically, but each individual's ability to build social status is suspended for some time after a reproduction event. Individuals preferentially copy the fertility of those around them according to the social status of those being copied. Thus in ABM II, social status is decoupled from fertility. In both models, two

weighting procedures are used: relative weighting and linear weighting. In ABM I, *relative weighting* refers to the fact that individuals of a given fertility preferentially copy those of a lower fertility, regardless of the exact fertility of the individual doing the copying. In this same model with linear weighting, the weight given to those whose fertility is being copied is an inverse linear function of their exact fertility. In ABM II, *relative weighting* refers to the fact that the fertility of those with a higher social status is copied preferentially to those with a lower social status. In linear weighting, the weight given to those whose fertility is being copied is an inverse linear function of their exact social status.

3.2 i. ABM I: Endogenous Social Status

Individuals occupy an $n \times n$ grid as before. The grid is sampled 2m times, where m is the total number of individuals, and when an individual is selected in a sampling event there is a 0.50 probability that either the conversion routine or the birth/death routine will be applied to this individual. The weight of conversion relative to birth/death can be modified by a parameter $p_{transmit}$, which gives the probability of the conversion routine being applied should it be chosen. When the birth/death procedure is called, the individual chosen reproduces according to their reproduction probability $p_{repr}(i,j)$, or dies according to a common mortality rate p_{death}. An individual's offspring are placed in one of the nearest-neighboring positions randomly. If the nearest-neighboring space is already occupied, the reproduction event does not take place. When the conversion routine is applied, the individual selected converts their reproduction probability to the average of their nearest neighbors. The boundary conditions are non-periodic.

If an individual is called on to convert, there is the possibility of copying error, such that this individual makes some error q in determining the average. Thus the resulting fertility lies marginally above or below the correct average ($r_{nb} \pm [q \times r_{nb}]$). r_{nb} is the average reproduction probability of the neighborhood, and q is a constant. The rate at which mutation occurs may also be adjusted by a parameter p_{mut}. As in the previous models, individuals of high fertility are underrepresented in the conversion process. This is accomplished by assigning high-fertility individuals a lower weight when calculating the average, thus the resulting average is a weighted average $\sum \frac{w_1 r_1 + w_2 r_2 + \cdots}{w_1 + w_2 + \cdots}$, where the r's are the reproduction probabilities of the nearest neighbors.

High-fertility individuals can be assigned a lower weight in a number of ways. We distinguish between two such weighting methods: relative weighting and linear weighting. Under the assumption of relative-weighting, if the neighbor to be included in the average has a higher fertility than the individual being converted, then they are assigned a weight of $a < 1$, whereas neighbors with a fertility less than or equal to the individual being converted have a weight of 1. In the linear weighting method, the weight with which a neighbor is considered is simply a linear function of the neighbor's reproduction rate, and this function does not depend on the reproduction rate of the individual being converted: $w_i = (-s \times r_i) + 1$, where s is a constant.

3.2 i. a. Relative Weighting

In this weighting procedure, high values of p_{death} result in ever increasing values of r_{ave}, the average reproduction probability of the population as whole. The simulation is stopped

when a single individual in the population exceeds a reproduction probability of 1- p_{death}. Intermediate values of p_{death} result in intermediate values of r_{ave}, with lower values of r_{ave} achieved for lower values of p_{death} in this range. A narrow range of r_{ave} is possible for this range of p_{death}. Low enough values of p_{death} result in ever decreasing values of r_{ave} until population crash (Figs 1 and 2).

The effects of other parameters on long-term r_{ave} of have been investigated (Figs 3, 4 and 5). The effects of the other parameters on long-term r_{ave} are comparable to those of the death rate. Intermediate values of p_{mut}, q, and *a* individually result in intermediate values of r_{ave}, with lower long-term r_{ave} achieved for lower values of these parameters in this range. High values of these parameters individually result in ever increasing r_{ave} to maximal levels. The simulations are stopped when a single individual exceeds a reproduction probability of 1 – p_{death}.

Lowering the value of $p_{transmit}$, the rate at which individuals undergo a conversion procedure, has an inverse of effect on the long-term r_{ave}. Low values of $p_{transmit}$ result in ever-increasing r_{ave} to maximal levels. As before, the simulations were stopped when a single individual exceeded a reproduction probability of 1-p_{death}. Intermediate values of $p_{transmit}$ result in intermediate long-term values of r_{ave}, with lower values corresponding to higher long-term r_{ave} in this range (Fig. 6).

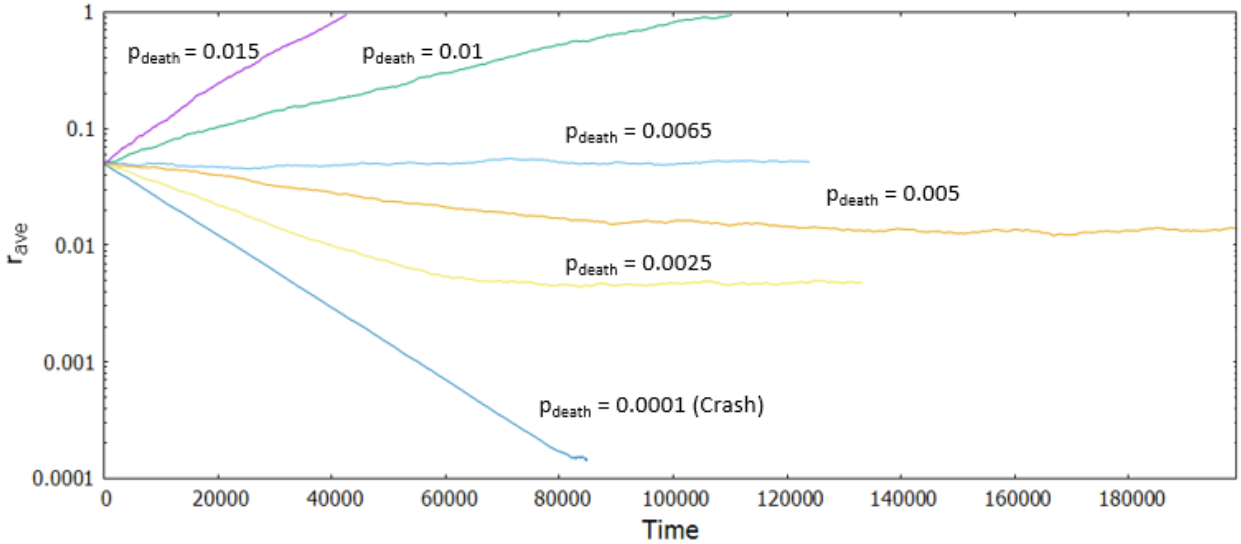

Fig. 1. Dynamics of average reproduction probability (r_{ave}) for six different death probabilities (p_{death}) assuming endogenous social status and relative weighting. Individuals adopt the weighted average of the fertility of those around them. A copying error occurs with a probability of p_{mut}. Individuals with a fertility greater than or equal to the individual taking the average are assigned a weight of 1 in the average. Individuals with fertility less than the individual taking the average are assigned a weight of *a*. Other parameters include the size of the copying error q and the rate at which individuals take the average ($p_{transmit}$). Parameter values: $p_{mut} = 0.01$; $q = 0.02$; $p_{transmit} = 0.001$; $a = 0.90$. The long term-reproduction probability is higher for high values of p_{death}. High values of p_{death} result in an ever-increasing r_{ave} to maximum values. Intermediate values of p_{death} result in intermediate values of r_{ave}. Low values of p_{death} result in ever decreasing values of r_{ave} leading to population crash.

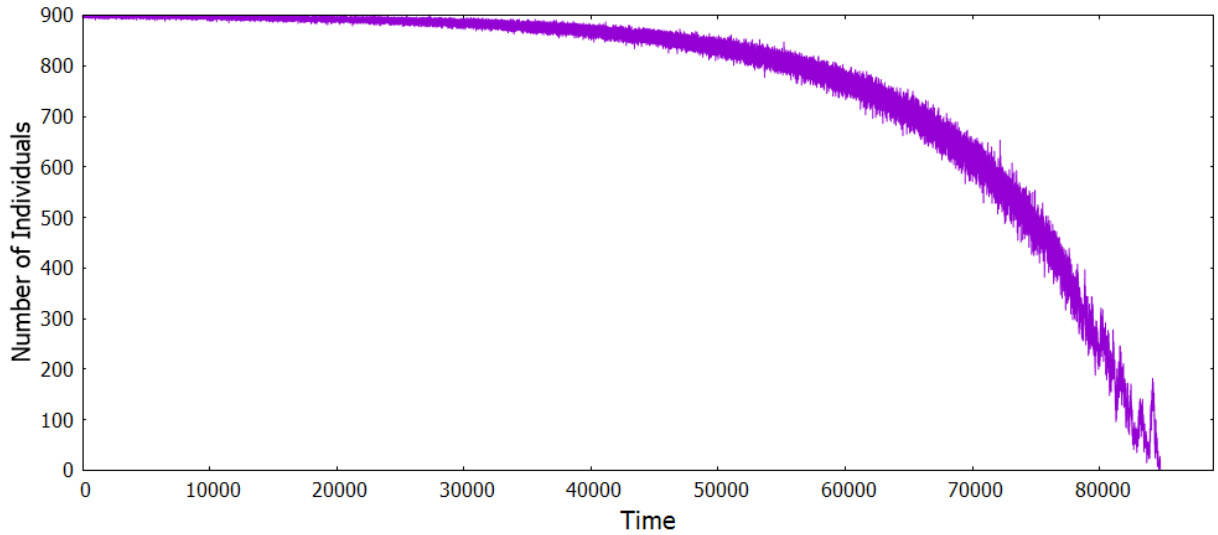

Fig. 2. Low values of mortality (p_{death}) result in ever decreasing values of average reproduction probability (r_{ave}) leading to population crash. Model assumes endogenous social status and relative weighting as in Fig. 1. Parameter values: $p_{mut} = 0.01$; $q = 0.02$; $p_{transmit} = 0.001$; $a = 0.90$; $p_{death} = 0.0001$.

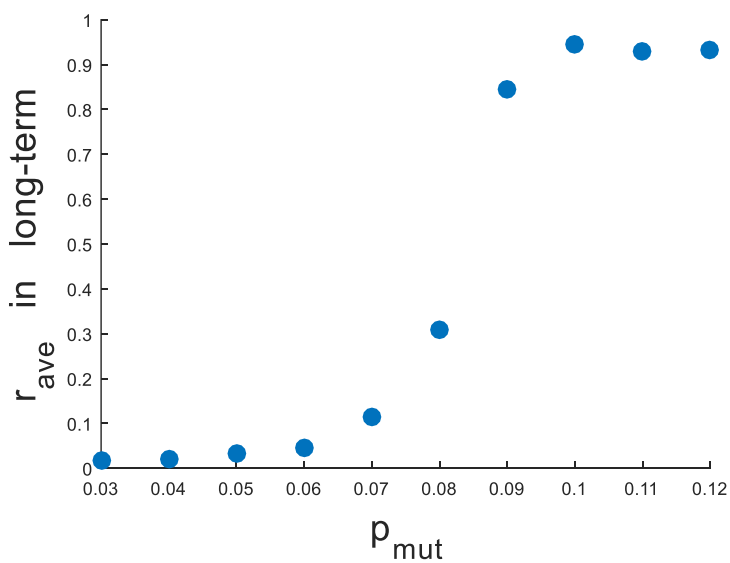

Fig. 3. Long-term average reproduction probability (r_{ave}) with respect to probability of copying error (p_{mut}) in model assuming endogenous social status and relative weighting. Individuals adopt the weighted average of the fertility of those around them. A copying error occurs with a probability p_{mut}. Individuals with a fertility greater than or equal to the individual taking the average are assigned a weight of 1 in the average. Individuals with fertility less than the individual taking the average are assigned a weight of *a*. Other parameters include the size of the copying error q, the rate at which individuals take the average ($p_{transmit}$), and the probability of death (p_{death}). r_{ave} in long-term increases with respect to p_{mut}. r_{ave} converges to intermediate values for intermediate values of p_{mut} and

increases to maximum values of for high values of p_{mut}. Other parameters: $p_{transmit} = 0.001$; $q = 0.025$; $a = 0.85$; $p_{death} = 0.005$.

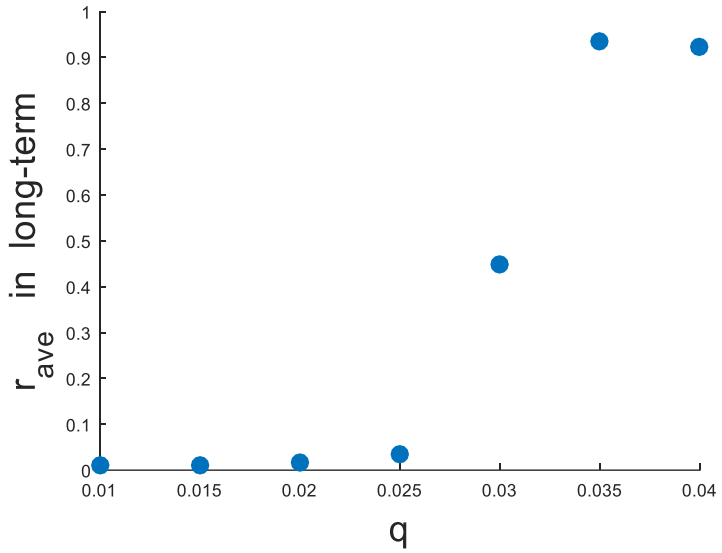

Fig. 4. Long-term average reproduction probability (r_{ave}) with respect to the size of copying error (q) in model assuming endogenous social status and relative weighting. Individuals adopt the weighted average of the fertility of those around them. A copying error occurs with a probability p_{mut}. Individuals with a fertility greater than or equal to the individual taking the average are assigned a weight of 1 in the average. Individuals with fertility less than the individual taking the average are assigned a weight of *a*. Other parameters include the rate at which individuals take the average ($p_{transmit}$) and the probability of death (p_{death}). r_{ave} in long-term increases with respect to q. r_{ave} converges to intermediate values for intermediate values of q and increases to maximum values of for high values of q. Other parameters: $p_{transmit} = 0.001$; $p_{mut} = 0.05$; $a = 0.85$; $p_{death} = 0.005$.

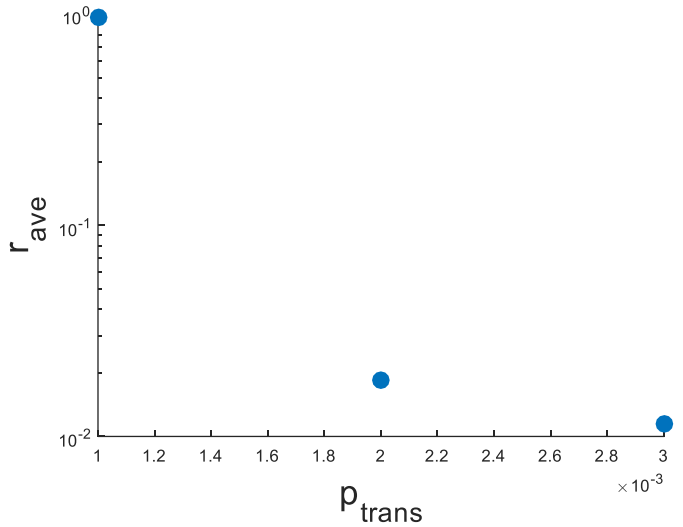

Fig. 5. Long-term average reproduction probability (r_{ave}) with respect to the rate of transmission ($p_{transmit}$) in model assuming endogenous social status and relative weighting. Individuals adopt the weighted average of the fertility of those around them with a probability $p_{transmit}$. A copying error occurs with a probability p_{mut}. Individuals with a fertility greater than or equal to the individual taking the average are assigned a weight of 1 in the average. Individuals with fertility less than the individual taking the average are assigned a weight of *a*. Other parameters include the size of the copying error q and the probability of death (p_{death}). r_{ave} in long-term decreases with respect to $p_{transmit}$. r_{ave} converges to intermediate values for intermediate values of $p_{transmit}$ and increases to maximum values for low values of $p_{transmit}$. Other parameters: $p_{mut} = 0.12$; $q = 0.01$; $a = 0.95$; $p_{death} = 0.005$.

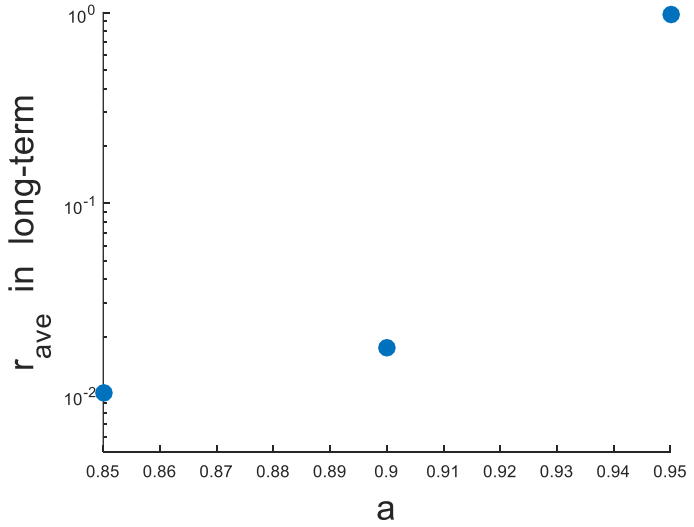

Fig. 6. Long-term average reproduction probability (r_{ave}) with respect to the weight of high fertility individuals in the average (a) in model assuming endogenous social status and

relative weighting. Individuals adopt the weighted average of the fertility of those around them. A copying error occurs with a probability p_{mut}. Individuals with a fertility greater than or equal to the individual taking the average are assigned a weight of 1 in the average. Individuals with fertility less than the individual taking the average are assigned a weight of *a*. Other parameters include the size of the copying error q, the rate at which individuals take the average ($p_{transmit}$), and the probability of death (p_{death}). r_{ave} in long-term increases with respect to a. r_{ave} converges to intermediate values for intermediate values of a. r_{ave} increases to maximum values for high values of a. Other parameters: $p_{transmit} = 0.001$; $p_{mut} = 0.12$; $q = 0.01$; $p_{death} = 0.005$.

3.2 i. b. Linear Weighting

In this weighting procedure, a continuum of long-term reproduction probabilities is possible. High mortalities result in high long-term r_{ave}, and low mortalities result in low long-term r_{ave}, with a continuum of results in between (Fig. 8). Very low p_{death} does not result in ever-decreasing r_{ave} that leads to a population crash as in the previous weighting method. Furthermore, p_{mut} and q do not have any effect on the long-term r_{ave} in this weighting method.

In this weighting method, $p_{transmit}$ and s both have an inverse relationship with long-term r_{ave} (Figs 9 and 10). Recall that $p_{transmit}$ is the rate at which individuals undergo a conversion procedure should the conversion routine be chosen, and s is the slope of the weighting function. High values of $p_{transmit}$ and s result in low long-term r_{ave}, and low $p_{transmit}$ and s result in high long-term r_{ave}, with a continuum of results in between.

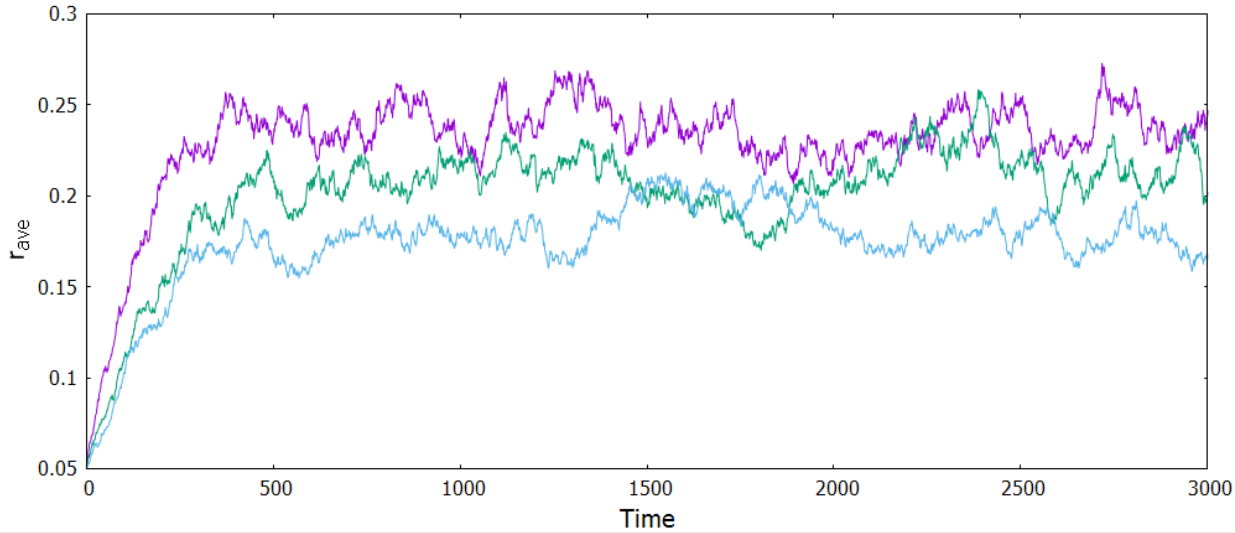

Fig. 7. Dynamics of average reproduction probability (r_{ave}) for three different death probabilities (p_{death}) in model assuming endogenous social status and linear weighting. Individuals adopt the weighted average of the fertility of those around them. A copying error occurs with a probability p_{mut}. The weight that an individual is assigned in the average is a linear function of their fertility ($w_i = (-s \times r_i) + 1$, where r_i is the reproduction probability of the neighbor and s is a constant). Other parameters include the size of the copying error q and the rate at which individuals take the average ($p_{transmit}$). Average reproduction probability in long-term decreases as p_{death} decreases. Purple: $p_{death} = 0.03$; Green: $p_{death} = 0.025$; Blue: $p_{death} = 0.02$. Other parameters: $p_{transmit} = 0.10$; $p_{mut} = 0.10$; $q = 0.04$; $s = 1.10$.

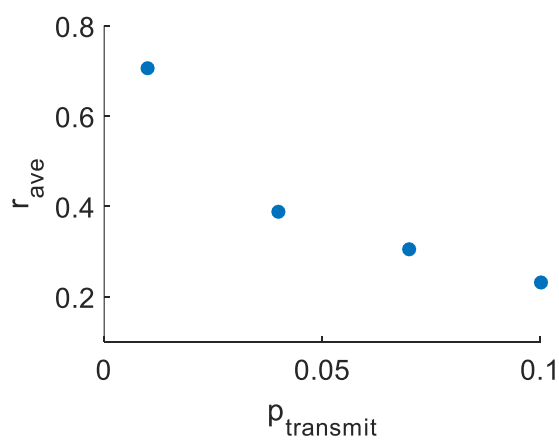

Fig. 8. Long-term average reproduction probability (r_{ave}) with respect to the rate of transmission ($p_{transmit}$) in model assuming endogenous social status and linear weighting. Individuals adopt the weighted average of the fertility of those around them. A copying error occurs with a probability p_{mut}. $p_{transmit}$ is the probability that the averaging procedure takes place. The weight that an individual is assigned in the average is a linear function of their fertility ($w_i = (-s \times r_i) + 1$, where r_i is the reproduction probability of the neighbor

and s is a constant). Other parameters include the size of the copying error q and the probability of death (p_{death}). r_{ave} decreases continuously with respect to $p_{transmit}$. Other parameters: s = 1.10; p_{mut} = 0.05; q = 0.06; p_{death} = 0.03.

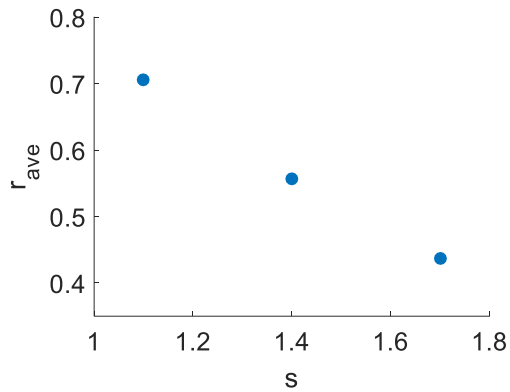

Fig. 9. Long-term average reproduction probability (r_{ave}) with respect to s in model assuming endogenous social status and linear weighting. Individuals adopt the weighted average of the fertility of those around them. A copying error occurs with a probability p_{mut}. The weight that an individual is assigned in the average is a linear function of their fertility ($w_i = (-s \times r_i) + 1$, where r_i is the reproduction probability of the neighbor and s is a constant). Other parameters include the size of the copying error q, the rate at which individuals take the average ($p_{transmit}$), and the probability of death (p_{death}). r_{ave} decreases continuously with respect to s. Other parameters: $p_{transmit}$ = 0.01; p_{mut} = 0.05; q = 0.06; p_{death} = 0.03.

3.2 ii. ABM II: Decoupled Social Status

In ABM II, individuals occupy an n × n grid as before. The grid is sampled 2m times at each iteration, where m is the total number of individuals occupying the grid. Each individual sampled has a 0.50 probability of undergoing a birth/death update or a social update. The birth/death procedure is the same as in ABM I. When the social update is applied, the chosen individual has a 0.50 probability of applying a social advancement procedure and a 0.50 probability of performing a conversion procedure. When the social advancement routine is applied, the individual undergoing the update increases their social status by 1. If

an individual reproduces, this individual cannot have the social advancement procedure applied to them for some fixed number of time steps w. When the conversion procedure is applied, the individual chosen converts their fertility to the weighted average of individuals in the neighborhood $\sum \frac{w_1 r_1 + w_2 r_2 + \cdots}{w_1 + w_2 + \cdots}$. The weight that a neighbor is given in the average depends on this neighbor's social status according to either linear weighting or relative weighting. Under the assumption of relative-weighting, if the neighbor to be included in the average has a lower social status than the individual being converted, then they are assigned a weight of $a < 1$, whereas neighbors with a social status greater than or equal to the individual being converted have a weight of 1. In the linear weighting method, the weight with which a neighbor is considered is a linear function of the neighbor's social status: $w_i = (s \times ss_i)$, where ss_i is the social status of the neighbor. Copying errors are applied the same as in ABM I.

3.2 ii. a. Relative Weighting

In this model, under the assumption of relative weighting, manipulating p_{death} has effects on the long-term r_{ave} comparable to ABM I. High rates of p_{death} result in ever increasing values of r_{ave} until maximal reproduction probability is achieved. Low to intermediate values of p_{death} result in relatively stable values of r_{ave} in the long-term, with lower values of p_{death} resulting in lower values of r_{ave} in this range. Low values of p_{death} do not result in ever-decreasing values of r_{ave} until population crash as in the relative weighted model of section 3.2 i. a. Increasing the rate of $p_{transmit}$ has the effect of lowering r_{ave} in the long-term. Very low values of $p_{transmit}$ can result in increasing values of r_{ave} to maximal reproduction, but

this increase does not appear to be the sort of threshold effect seen in section 3.2 i. a. or when increasing values of p_{death} in this section. Increasing the value of *a* results in higher long-term values of r_{ave} when equilibria are achieved. High values of *a* can result in maximal reproduction as well, but this again does not appear to be a threshold phenomenon.

Changing the values of p_{mut} or q has no effect on the long-term average values of r_{ave} in the long-term when equilibria are achieved, although the behavior of the time series is more erratic for high values of either parameter. If equilibria are not achieved, the r_{ave} increases until maximal reproduction probability. The values of p_{mut} or q that achieve this outcome have no obvious pattern or directionality. (Results not shown)

Changing the value of w has an effect unique among all the parameters. Increasing w decreases the long-term r_{ave} up to a certain value. Beyond this value, maximal reproduction probability is achieved in the long-term.

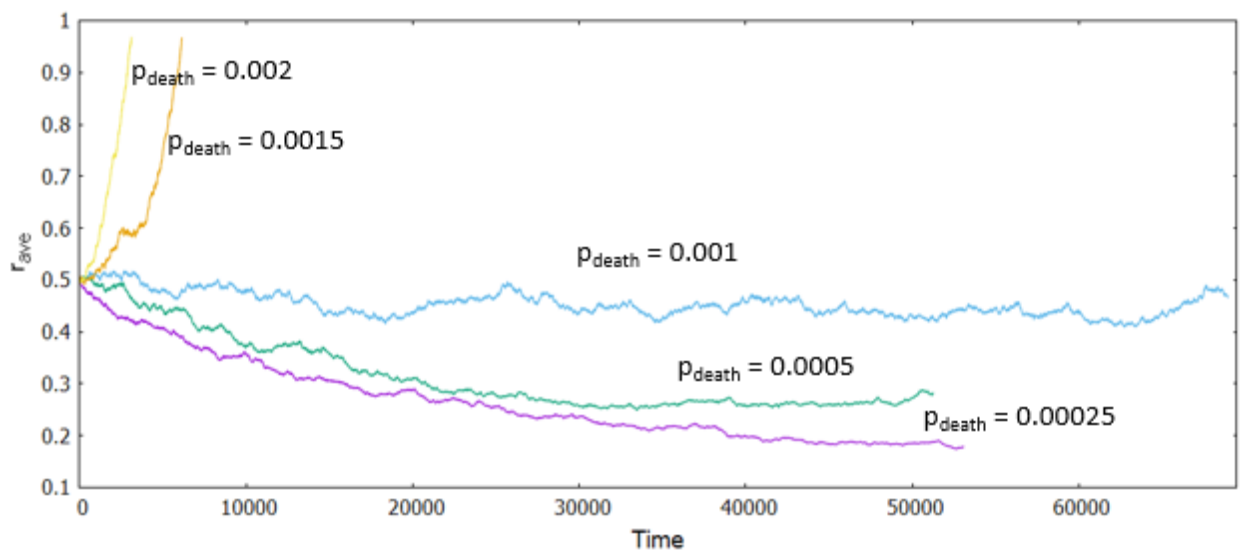

Fig. 10. Dynamics of the average reproduction probability (r_{ave}) with six different death probabilities (p_{death}) in model assuming decoupled social status and relative weighting. Individuals adopt the weighted average of the fertility of those around them. A copying

error occurs with a probability of p_{mut}. Individuals with a social status greater than or equal to the individual taking the average are assigned a weight of 1 in the average. Individuals with social status less than the individual taking the average are assigned a weight of *a*. Social status is built stochastically. When an individual reproduces, they must wait for some time-period w before they can build social status. Other parameters include the size of the copying error q and the rate at which individuals take the average ($p_{transmit}$). The long term-reproduction probability is higher for high values of p_{death}. High values of p_{death} result in an ever-increasing r_{ave} to maximum values. Lower values of p_{death} result in stable levels of r_{ave}. The equilibrium levels of r_{ave} decrease with decreasing levels of p_{death}. Other parameters: $p_{mut} = 0.02$; $q = 0.02$; $p_{transmit} = 0.003$; $a = 0.40$; $w = 5$.

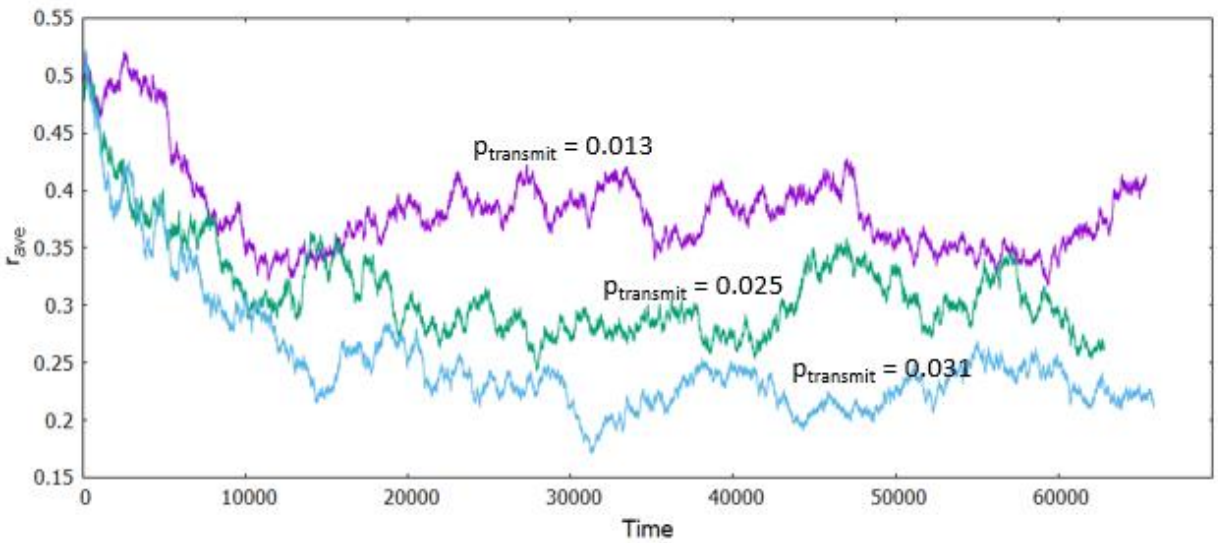

Fig. 11. Dynamics of average reproduction probability (r_{ave}) for three different rates of transmission ($p_{transmit}$) in model assuming decoupled social status and relative weighting. Individuals adopt the weighted average of the fertility of those around them. A copying error occurs with a probability of p_{mut}. $p_{transmit}$ is the probability that the averaging procedure takes place. Individuals with a social status greater than or equal to the individual taking the average are assigned a weight of 1 in the average. Individuals with social status less than the individual taking the average are assigned a weight of *a*. Social status is built stochastically. When an individual reproduces, they must wait for some time-period w before they can build social status. Other parameters include the size of the copying error q and the probability of death (p_{death}). r_{ave} in long-term decreases with respect to $p_{transmit}$. r_{ave} converges to intermediate values for intermediate values of $p_{transmit}$ and increases to maximum values for low values of $p_{transmit}$. Other parameters: $p_{mut} = 0.02$; $q = 0.02$; $p_{death} = 0.02$; $a = 0.40$; $w = 2$.

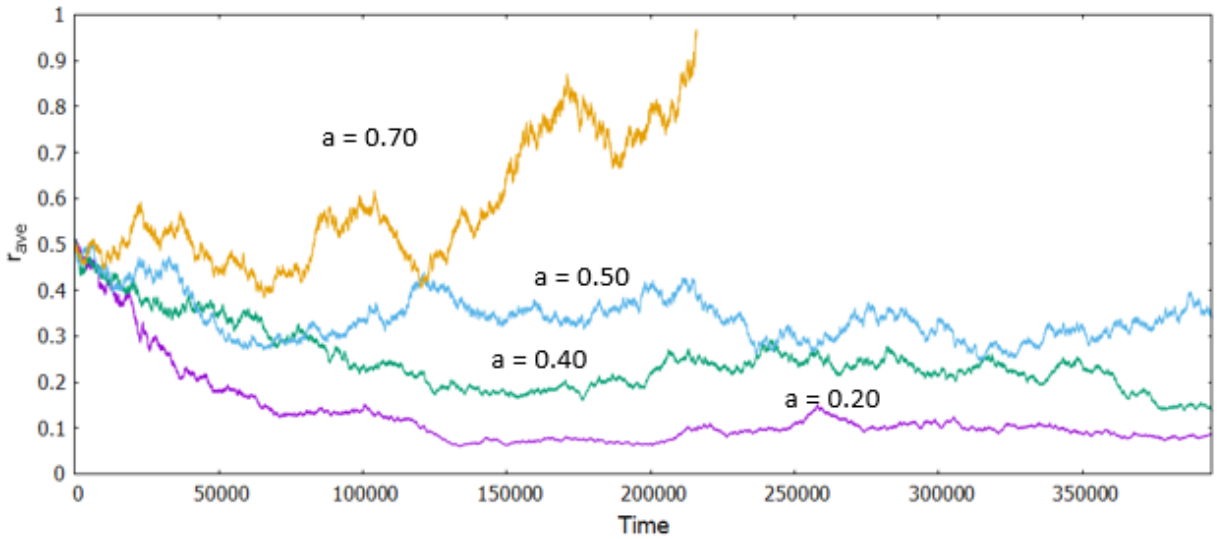

Fig. 12. Dynamics of average reproduction probability (r_{ave}) for four different values of *a* in model assuming decoupled social status and relative weighting. Individuals adopt the weighted average of the fertility of those around them. A copying error occurs with a probability of p_{mut}. Individuals with a social status greater than or equal to the individual taking the average are assigned a weight of 1 in the average. Individuals with social status less than the individual taking the average are assigned a weight of *a*. Social status is built stochastically. When an individual reproduces, they must wait for some time-period w before they can build social status. Other parameters include the size of the copying error q, the rate at which individuals take the average ($p_{transmit}$), and the probability of death (p_{death}). r_{ave} converges to intermediate values for intermediate values of a. r_{ave} in long-term increases with respect to a. r_{ave} increases to maximum values for high values of a. Other parameters: $p_{transmit} = 0.07$; $p_{mut} = 0.02$; $q = 0.02$; $p_{death} = 0.001$; $w = 2$.

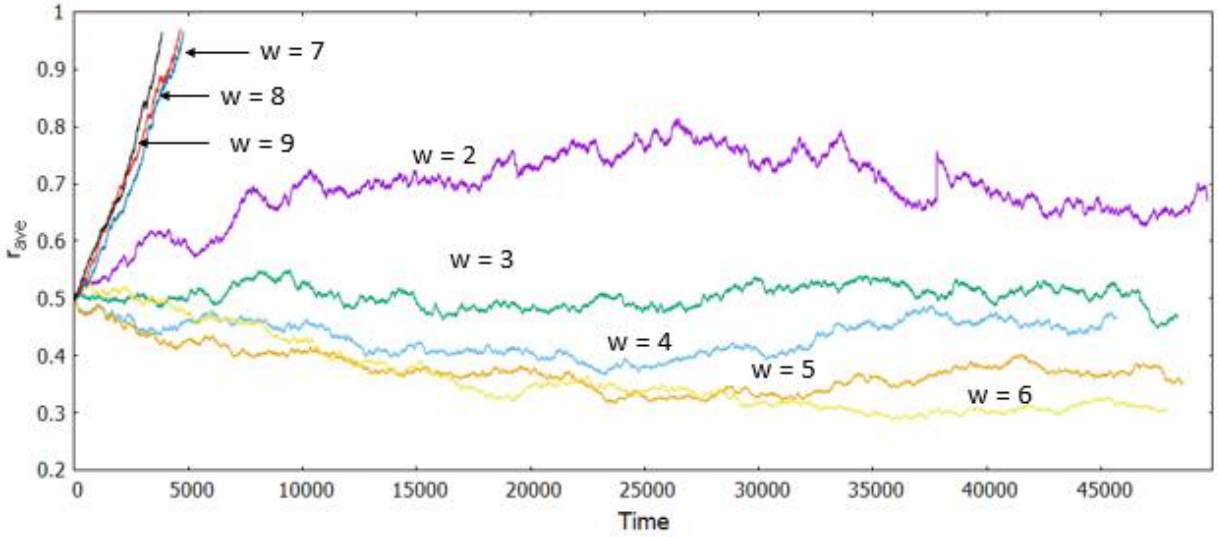

Fig. 13. Dynamics of average reproduction probability (r_{ave}) for different values of w in model assuming decoupled social status and relative weighting. Individuals adopt the weighted average of the fertility of those around them. A copying error occurs with a probability of p_{mut}. Individuals with a social status greater than or equal to the individual taking the average are assigned a weight of 1 in the average. Individuals with social status less than the individual taking the average are assigned a weight of *a*. Social status is built stochastically. When an individual reproduces, they must wait for some time-period w before they can build social status. Other parameters include the size of the copying error q, the rate at which individuals take the average ($p_{transmit}$), and the probability of death (p_{death}). Long-term average reproduction probability decreases with respect to w with diminishing effect up to a certain threshold. Setting w beyond this threshold results in ever increasing reproduction probability until maximal reproduction probability is achieved. Other parameters: $p_{transmit} = 0.004$; $p_{mut} = 0.02$; $q = 0.02$; $p_{death} = 0.001$; $a = 0.40$.

3.2 ii. b. Linear Weighting

Lowering p_{death} in ABM II under the assumption of linear weighting has an effect comparable to ABM I under linear weighting. Lower values of p_{death} result in lower long-term values of r_{ave}. Increasing the rate of $p_{transmit}$ had an inverse effect on the long-term values of r_{ave}. Increasing w decreases the long-term values of r_{ave}, but this effect diminishes as w increases. Very high values of w result in ever increasing r_{ave} until maximal

reproduction probability is achieved. Adjusting p_{mut}, q, and s did not have an effect on the average long-term value of r_{ave}.

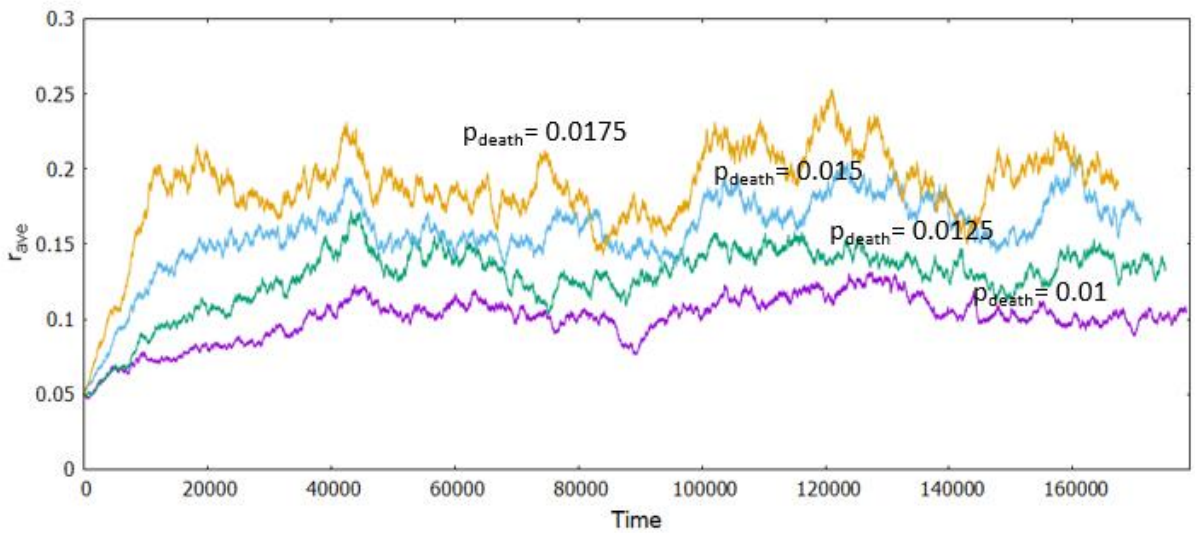

Fig. 14. Dynamics of average reproduction probability (r_{ave}) for four different death probabilities (p_{death}) in model assuming decoupled social status and linear weighting. Individuals adopt the weighted average of the fertility of those around them. A copying error occurs with a probability of p_{mut}. The weight that individuals are assigned in the average is a linear function of their social status ($w_i = (s \times ss_i)$, where ss_i is the social status of the neighbor, and s is a constant). Social status is built stochastically. When an individual reproduces, they must wait for some time-period w before they can build social status. Other parameters include the size of the copying error q and the rate at which individuals take the average ($p_{transmit}$). Average reproduction probability in long-term decreases as p_{death} decreases. Other parameters: $p_{transmit} = 0.07$; $p_{mut} = 0.02$; $q = 0.02$; $s = 0.01$; $w = 2$.

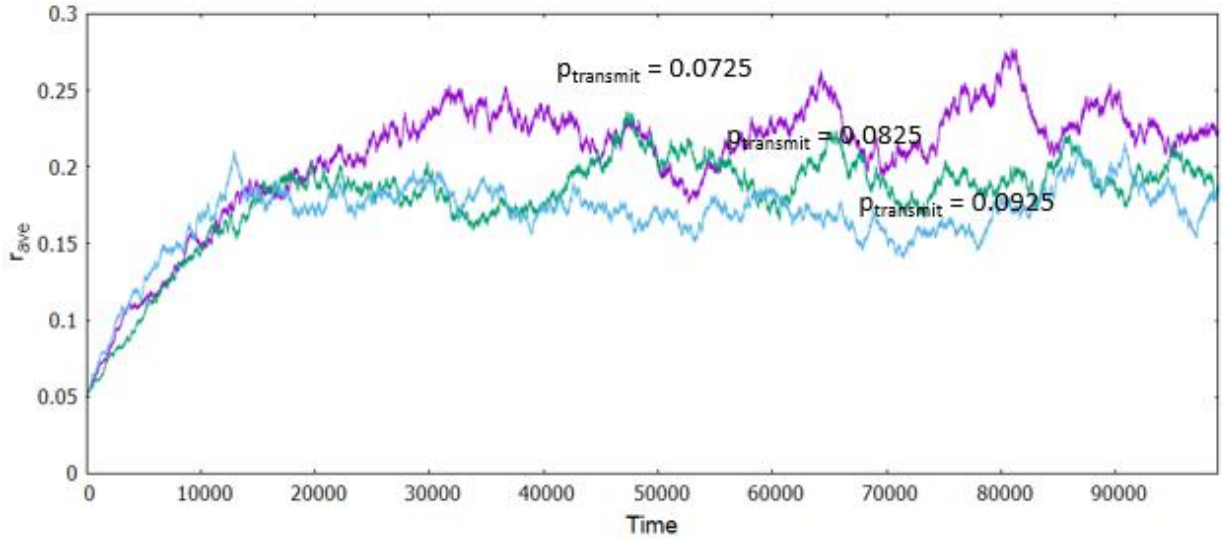

Fig. 15. Dynamics of average reproduction probability (r_{ave}) for different rates of transmission ($p_{transmit}$) in model assuming decoupled social status and linear weighting. Individuals adopt the weighted average of the fertility of those around them. A copying error occurs with a probability of p_{mut}. The weight that individuals are assigned in the average is a linear function of their social status ($w_i = (s \times ss_i)$, where ss_i is the social status of the neighbor, and s is a constant). Social status is built stochastically. When an individual reproduces, they must wait for some time-period w before they can build social status. Other parameters include the size of the copying error q, the rate at which individuals take the average ($p_{transmit}$), and the probability of death (p_{death}). r_{ave} in long-term decreases continuously with respect to $p_{transmit}$. Other parameters: $s = 0.01$; $p_{mut} = 0.02$; $q = 0.02$; $p_{death} = 0.02$; $w = 2$.

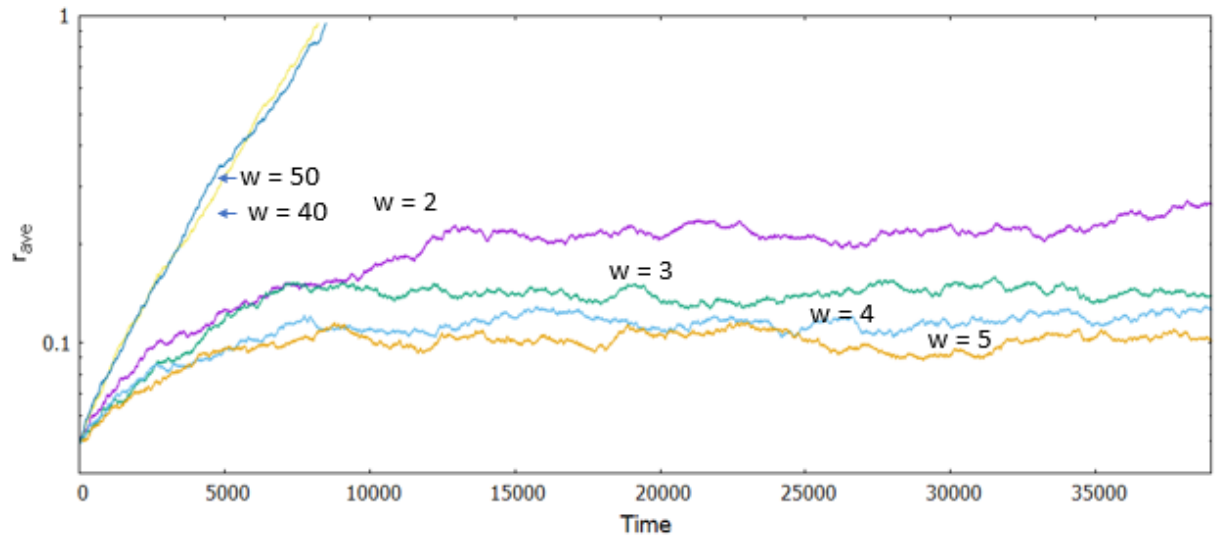

Fig. 16. Dynamics of average reproduction probability (r_{ave}) for different values of w in model assuming decoupled social status and linear weighting. Individuals adopt the weighted average of the fertility of those around them. A copying error occurs with a probability of p_{mut}. The weight that individuals are assigned in the average is a linear function of their social status ($w_i = (s \times ss_i)$, where ss_i is the social status of the neighbor, and s is a constant). Social status is built stochastically. When an individual reproduces, they must wait for some time-period w before they can build social status. Other parameters include the size of the copying error q, the rate at which individuals take the average ($p_{transmit}$), and the probability of death (p_{death}). r_{ave} in the long-term decreases as w increases. The effect of increasing w diminishes at higher values. r_{ave} increases to maximal values if w is beyond a certain threshold. Other parameters: $p_{transmit} = 0.07$; $s = 0.01$; $p_{mut} = 0.02$; $q = 0.02$; $p_{death} = 0.02$.

3.3 Discussion

Some patterns of outcome with respect to changing parameters are intuitive, while others are not. For example, in all models, as $p_{transmit}$ is increased, r_{ave} is decreased. In all models with relative weighting, decreasing parameter a, the weight that higher fertility individuals are given in the average, has the effect of increasing the long-term r_{ave}. One might not predict that increasing p_{mut}, the rate of mutation, or q, the size of the mutation, would increase long-term r_{ave} in ABM I under the assumption of relative weighting, but

have no effect on long-term r_{ave} in ABM I with linear weighting or either weighting procedure in ABM II. One might expect s, the slope of the weighting function in the linear weighting assumption, to have a negative effect on the long-term r_{ave} under either the assumptions of ABM I or ABM II. While increasing s did have this effect in ABM I, changing s had no effect on the long-term r_{ave} in ABM II. These observations highlight the importance of comparing models with different assumptions, however trivial the differences may seem. Another parameter of interest was w, the amount of time an individual has to wait after reproducing to continue building social status. As w increases, the long-term r_{ave} decreases up to a certain value of w, beyond which r_{ave} instead increases to maximal values. This threshold effect is caused by the fact that, depending on initial conditions, the variation of individual reproduction events is not great enough to include any individual that would delay reproduction by w to have a social advantage and be emulated.

We considered nearest neighbor interactions. Not only could the assumption of perfect mixing be investigated, but more complex, random, or realistic types of interactions could be explored as well. Sexual reproduction was incorporated into the models but did not produce any qualitative differences in results, thus these results were not included. A social status building procedure was considered in ABM II in order to somewhat decouple reproduction from social status, but it is still assumed that it is fertility itself that is copied. This may be justified if it is assumed that there is a value system or preference map that is adopted in developed countries that results in low fertility, and it is this value system or preference map that is transmitted (Lesthaege, 1983). Furthermore, it has been shown that individuals' values, beliefs, and behaviors are adopted by others according to their social

status, even when the traits adopted have no obvious logical connection to the social status of the individuals being copied (Henrick and Gil-White 2001; Hendrick, 2008).

In ABM II, the social status building routine is minimalistic. Its only function is to decouple social status from fertility. Individuals' fertility is copied according to social status, and reproduction limits one's ability to build social status. One could explore a more detailed model in which some of an individual's social status is inherited from parents, the size of this inheritance effects their future ability to accrue resources, and individuals vary in the extent to which they allocate resources to building social status or having children (Hill and Reeve, 2005). In addition, one could investigate outcomes of a model which allows this choice in allocation to be different between the sexes, as has been modeled elsewhere (Hopcroft and Whitmeyer, 2011). Mate selection could also be incorporated into the model such that the sexes differ in choosiness with respect to social status. Incorporating these details could produce patterns emerging in the literature of a near universal negative relationship between social status and fertility for women and an occasionally positive relationship for men in modern societies (Feider and Huber, 2007; Hopcroft, 2015).

Arguably the most important result of this study is that long-term average reproduction probability is lower at lower mortality rates in all models. This outcome is consistent with a phenomenon often noted by demographers, that fertility transitions are difficult to initiate in the absence of a mortality decline (Mason, 1997). Lowering the mortality rate increases the population density, which increases the frequency of contacts between individuals, resulting in a greater rate of transmission relative to reproduction. If low fertility individuals are overrepresented in the transmission process, then fertility

should decrease as the population density increases. Thus this work provides a mechanism for the general pattern of the demographic transition of the 19th and 20th centuries. One prediction that follows from the mechanism proposed by the model is that fertility should be lower in areas of high population density. This does in fact appear to be the case (Lutz et al. 2006). Another important observation from the models, given some assumptions, is that a low enough mortality rate results in an ever-decreasing r_{ave}, such that a population crash results. Western European countries have seen below replacement fertility for some time (Castles and Francis, 2003; Golstein et al. 2003). Also, ideal family size among young adults in German speaking countries is below replacement level, suggesting that such a trend is likely to continue in the future. Such observations may result from the type of cultural evolutionary dynamics explored in this project.

References

Alvergne, A., Lummaa, V. 2014. Ecological variation in wealth-fertility relationships in Mongolia: the central theoretical problem of sociobiology not a problem after all. Proc Biol Sci 281(1796):20141733.

Borgerhoff Mulder, M. 1997. Brothers and sisters: How sibling interactions affect optimal parental allocations. Human Nature 9(2):119-162.

Castles, F. G., Fancis, G. 2003. The world turned upside down: below replacement fertility, changing preferences and family-friendly public policy in 21 OECD countries. Journ Euro Social Pol 13:209-227.

Cavalli-Sforza, L. L., Feldman, M. W. 1981. "Cultural Transmission and Evolution: A Quantitative Approach." Princeton: Princeton University Press.

Chagnon, N. A. 1988. Life history, blood revenge and warfare in a tribal population. Science 985-992.

Cleland, J., Wilson, C. 1987. Demand theories of the fertility transition: an iconoclastic view. Pop Stud 41(1):5-30.

Cohen, J. E., Kravdal, O., Keilman, N. 2011. Childreaing impeded education more than education impeded childbearing among Norwegian women. Proc Natl Acad Sci U S A 108(29):11830-11835.

Creanza, N., Kolodny, O., Feldman, M. W. 2017. Cultural evolutionary theory: how culture evolves and why it matters. PNAS 114(30):7782-7789.

Fieder, M., Huber, S. 2007. The effects of sex and childlessness on the association between social status and reproductive output in modern society. Evol and Hum Beh 28:392-398.

Fieder, M., Huber, S., Bookstein, F. L., Iber, K., Schafer, K., Winckler, G., Wllner, B. 2005.

Status and reproduction in humans: New evidence for the validity of evolutionary explanations on basis of a university sample. Ethology 111:940-950.

Fogarty, L., Creaenza, N., Feldman, M. W. 2013. The role of cultural tranmission in human demographic change: an age-structured model. Theor Pop Biol 88:68-77.

Goldstein, J., Lutz, W., Testa, M. R. 2003. The emergence of sub-replacement family size ideals in Europe. Pop Res and Pol Rev 22:479-496.

Henrich, J. 2008. Cultural transmission and the diffusion of innovations: adoption dynamics indicate that biased cultural transmission is the predominate force in behavioral change. Am. Anthrop 103(4):992-1013.

Henrich, J., Gil-White, F. 2001. The evolution of prestige. Evol and Hum Behav 22(3):165-196.

Hill, S. E., Reeve, H. K. 2005. Low fertility in hymans as the evolutionary outcome of snowballing resource games. Behav Evol 16(2):398-402.

Hopcroft, R. 2015. Sex differences in the relationship between status and number of offspring in the contemporary U.S. Evol Hum Beh 36:146-151.

Hopcroft, R., Whitmeyer, J. 2011. A choice model of occupational status and fertility. Journ Math Sociol 34(4):283-300.

Ihara, Y., Feldman, M. W. 2004. Cultural niche construction and the evolution of small family size. Theor Pop Biol 65:105-111.

Kaplan, H. S., Lancaster. J. B., Johnson, S. E., Bock, J. A. 1995. Does observed fertility maximize fitness among New Mexican men? Human Nature 6:325-360.

Kaptijn, R. Thomese, F. van Tilburg, T. G., Liefbroer A. C., Deeg, D. J. H. 2010. Low fertility in contemporary humans and the mate value of their children: sex-specific effects on social

status indicators. Evolution and Human Behavior 31:59-68.

Kirk, D. 1996. Demographic transition theory. Pop Stud 50(3):361-387.

Knodel, J., van de Walle, E. 1979. Lessons from the past: policy implications of historical fertility studies. Popul and Devel Rev 5(2):217-245.

Lawson, D. W., Mace, R. 2011. Parental investment and the optimization of human family size. Phil trans Royal Soc *B* 333-343.

Lesthaeghe, R. A. 1983. A century of demographic and cultural change in Western Europe: an exploration of underlying dimensions. Popul Dev Rev 9:411-435.

Mason, K. O. 1997. Explaining fertility transitions. Demography 34(4):443-454.

Notestein, Frank W. 1945. Population - the long view. In *Food for the World*, by T.W. Schultz. ed., 36-57. Chicago: University of Chicago Press.

Perusse, D. 1993. Cultural and reproducctive succes in industrial societies: test relationships at the proximate and ultimate levels. *Behav Brain Sci* 16:267-322.

Rogers, A. R. 1990. Evolutionary economics of human reproduction. *Ethology and Sociobiology* 11(6):479-495.

Skirbekk, V. 2008. Fertility trends by social status. *Demo Res.* 18:145-180.

Thompson, W. 1929. Population. *Am Journ of Sociol* 34:959-75.

Vining, D. R. 1986. Social versus reproductive success--the central theoretical problem of human sociobiology. *Behav Brain Sci* 9:167-260.